

51  
Photopolarimetric studies of comet P/Halley

and

some astronomical objects

043  
SEN

1425P

✓

BY

Asoke Kumar Sen

Physical Research Laboratory

Ahmedabad 380 009

India

A Thesis

Submitted to

Gujarat University

For the Degree of

Doctor of Philosophy

July 1990

043



B14251

**Dedicated to**

**.....my parents**

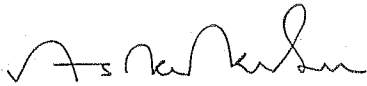
**and**

**.....my wife**

Certificate

I hereby declare that the work presented in this thesis is original and has not formed the basis for the award of any degree or diploma by any University or Institution.

Author



Asoke Kumar Sen

Physical Research Laboratory

Ahmedabad 380 009, India.

Certified by



Professor M. R. Deshpande

Physical Research Laboratory

Ahmedabad 380 009, India.

## Abstract

Chapter 1, gives an overview and an introduction of cometary studies in general.

In chapter 2, the instruments used for making the photopolarimetric observations used in the present work are discussed. A two channel photopolarimeter which works on a rapid modulation principle was used. The sampling rate of the instrument is 2-ms and the data are processed on-line with a Z-80 microprocessor. This instrument was mounted on the Cassegrain focus of one-meter telescope at Vainu Bappu observatory, Kavalur and the comet was observed for seven nights (9-10th Dec 1985, 15-19th March 1986) for photometry and polarimetry. In addition to this, a wide field imaging polarimetry of comet P/Halley was carried out on Jan 5 1986 (almost a month before it's perihelion). A Celestron-14" telescope at Gurushikhar observatory, Mount Abu was used for these observations.

In Chapter 3, the results from the photometric studies made on comet P/Halley are presented. The absolute fluxes in different emission bands (CN,  $C_3$ ,  $CO^+$ ,  $C_2$  and  $H_2O^+$ ) were calculated along with the background solar continuum flux in order to provide supporting data for the molecular band polarization calculations which are given in Chapter 4. For the coma region it has been found that  $C_2$  emission is stronger than CN and  $C_3$ , whereas CN and  $C_3$  are almost equal. In addition  $CO^+$  and  $H_2O^+$  fluxes are found to be equal and they exhibit weaker emission compared to other emission bands. Among the three neutral molecules, CN,  $C_3$  and  $C_2$ , it has been found that  $C_3$  emission decreases fastest along the



cometary tail and  $C_2$  decreases slightly faster than CN. Also the production rates of different neutral molecules were calculated.

In Chapter 4, we discuss the results obtained on the band polarization of the molecules CN,  $C_3$ ,  $CO^+$ ,  $C_2$  and  $H_2O^+$  where the emission takes place by resonance fluorescence mechanism. Using Stokes parameters, calculations were done for the resonance fluorescence polarization values in different emission bands. It has been found that emissions from CN,  $C_2$  and  $C_3$  have polarization values between 5-7%, at a phase angle of 66.1 degree. For CN and  $C_2$  the polarization values agree well with the theoretically predicted values, but for  $C_3$  the polarization value falls much below the theoretically predicted value. The two ionic molecules  $CO^+$  and  $H_2O^+$  show large polarizations, 17.5% and 29.5% respectively.

Chapter 5, describes the imaging polarimetry work done on the comet P/Halley, which is an excellent tool for probing cometary nuclear activities. Comet P/Halley was imaged polarimetrically in the coma and tail region on January 5, 1986. In the inner coma a small region has been found which has very low ( $< 2\%$ ) polarization. But in the tailward direction beyond the outer coma ( $> 10^5$  km) two separate regions of enhanced polarizations ( $> 8\%$ ) were found. We showed that the high polarization in those regions can be possible by the presence of small size grains as compared to the neighboring regions. The small grains were perhaps pocketed there by some nuclear jet activities. The low polarization region in the inner coma, can also be connected with a fresh dust jet ejected from the nucleus, so that the dust density is still high enough to cause multiple scattering. The low polarization could be

resulting from multiple scattering in the region of high dust concentration, in the fresh ejecta.

In Chapter 6, we discuss results on continuum filter polarimetry of comet P/Halley and properties of cometary dust. Comet P/Halley was observed polarimetrically for seven nights in IHW and other continuum filters, during its pre and post perihelion passages. The observed polarization increases with the wavelength at large phase angle values and the nature of the wavelength dependence of polarization is different for the different parts of the comet, signifying the segregation of different size grains over different parts of the comet. These polarimetric observations have been combined with the observations taken by other investigators, to get a complete picture of phase angle and wavelength dependence of polarization of comet P/Halley.

Assuming spherical shaped particles (with density  $\rho = 1.0$ ), and using the dust size distribution functions obtained by the Vega and Giotto spacecraft, we have calculated, by applying Mie scattering theory, the complex values of the refractive indices of the cometary grains.

In chapter 7 we briefly describe some of the polarimetric works done on the symbiotic peculiar star R Aquari and a set of four supergiant stars.

## Acknowledgement

It is a pleasure to express my gratitude to Professor M. R. Deshpande, who in addition to providing useful advice, guidance and encouragement, made the work a source of joy and excitement. I also express my sincere gratitude to Dr. U. C. Joshi, for useful scientific discussions and providing me various helps, during the last six years. I am grateful to Professors P. V. Kulkarni and S.P. Pandya for their interest and encouragement in this work. Sincere gratitudes to Professor J.N. Desai for useful scientific discussions. I am grateful to Professor R. K. Verma, Director, PRL, for his encouragement in this work. I am also grateful to Prof. N.K. Rao and Dr. A.V. Raveendran of IIA Bangalore, for useful scientific discussions.

My special thanks to Ms. C. R. Shah and Mr. A. B. Shah for providing me all the possible computer hardware and software facilities required for this work. Mr. N.M. Vadher provided all the helps at the time of observations, which are sincerely acknowledged. Sincere thanks to Mr. Banshidhar, Mr. N. F. Khoja, and Mr. V.D. Patel for their various helps during the last six years.

I am thankful to all my friends in the hostel for providing me, nice company during the last six years.

List of publications of Asoke Kumar Sen

---

published papers

1. "Variation of linear polarization in the R Aquarii system"- Deshpande, M.R., Joshi, U.C., Kulshrestha, A.K., Sen, A.K., Rao, N.K., and Raveendran, A.V., 1987, Publication of Astrophysical Society of Pacific, Vol 99, p 62.

2. "Polarization investigations in four peculiar supergiants with high IR excess"- Joshi, U.C., Deshpande, M.R., Sen, A.K., and Kulshrestha, A.K., 1987, Astronomy and Astrophysics, Vol 181, p31.

3. "Polarimetric observations of comet P/Halley on 19 March 1986"- Sen, A.K., Joshi, U.C., Deshpande, M.R., Kulshrestha, A.K., Babu, G.S.D., and Shylaja, B.S., 1988, Astronomy and Astrophysics, Vol 204, p317.

4. "Molecular band polarization in comet P/Halley."- Sen, A.K., Joshi, U.C., and Deshpande, M.R., 1989, Astronomy and Astrophysics, Vol. 217, p307.

5. "Imaging polarimetry of comet P/Halley"- Sen, A.K., Joshi, U.C., Deshpande, M.R., and Debi Prasad, C., 1990, Icarus (in press), to appear in July issue.

6. "Polarimetry of comet P/Halley: properties of dust"- Sen, A.K., Deshpande, M.R., Joshi, U.C., Rao, N.K., and Raveendran, A.V., 1990, submitted to Astronomy and Astrophysics.

7. "Photometry of comet P/Halley" -Sen, A.K., Deshpande, M.R., and Joshi, U.C., 1990, submitted to Bulletin of Astronomical Society of India.

Papers Presented in Conference/ Seminar/ Workshop etc.

1."Photopolarimetric observations of comet P/Halley on 19 th March"- Sen, A.K., Joshi, U.C., Deshpande, M.R., Kulshrestha, A.K., and Sivaraman, K.R., Physics Teacher, Jan-March 1988. Proc. of the 5th Young Physicists' Coll. Calcutta, 17-19 August, 1987.

2."Study of Debye Waller factor using two parameter lattice model"- Sen, A.K., Tolpadi, S., and Mathur, B.K.; in the Physics section of Indian Science Congress, Lucknow, January 3-8, 1985.

3."Polarization studies in Bok globules and evidence for star formation"- Joshi, U.C., Kulkarni, P.V., Deshpande, M.R., Sen, A. K., and Kulshrestha, A.K.; in International Astronomical Union, Symposium No 122, Heidelberg, June 23-27, 1986.

4."Photopolarimetric observations of comet p/Halley on 19 March"- Sen, A.K., Joshi, U.C., Deshpande, M.R., Kulshrestha, A. K., and Sivaraman, K.R.; Bul. Astron. Soc. of India. Vol 15, No 1, p23, Proc. of the annual meeting of Astronomical Society of India, Bangalore, 9-12 December, 1986

5."Polarimetric observations of p/Halley."- Rao, N.K., Raveendran, A. V., Sen, A.K., Joshi, U.C. and Deshpande, M.R., Proc. of the National symposium on comet Halley, Bangalore 27-29, 1987.

6."Polarimetric investigations of some peculiar supergiants"- Joshi, U.C., Deshpande, M.R., Sen, A.K., and Kulshrestha, A.K.; Bul. Astron. Soc. of India. Vol 15, No 1, p23, Proc. of the annual meeting of Astronomical Society of India, Bangalore, 9-12 December, 1986

7."Polarimetry of SN1987A"-Sen, A.K., Joshi, U.C., Deshpande,

M.R., ; Bull. of Astron. Soc. of India. Vol 16, No.2-3, p86, Proc. of the annual meeting of the Astronomical Society of India, Raipur, 11-14 Dec, 1987.

8."Polarimetry of SN 1987A-A dust shell model"-Joshi, U.C., Sen, A.K., Deshpande, M.R., and Kulshrestha, A.K.; in International Astronomical Union General Assembly Meeting (comission 25), Baltimore 1988.

9."Do elliptical galaxies harbour BL Lac objects ?"- Deshpande, M.R., Joshi, U.C., Sen, A.K., and Kulshrestha, A.K.; in Observational Astrophysics with high precissional data, p 159, 1987, Proc. of 27th Liege International Astronomical Union Colloquium , June 23-26, 1987.

10."Optical polarization of active galactic nuclei"- Deshpande, M.R., Kulshrestha, A.K., Joshi, U.C., and Sen, A.K., in 27th Liege International Astronomical Colloquium, June 23-26, 1987.

11."Polarimetry of Supernova 1987A-A dust shell model"- Joshi, U.C., Sen, A.K., Deshpande, M.R. and Rekha Jain, Kodaikanal Observatory Bull. 10, p43, 1988.

## C O N T E N T S

### Chapters

1. Introduction	1
2. Instrumentation and observation	14
3. Photometry of comet P/Halley	31
4. Molecular band polarization in comet P/Halley	43
5. Imaging polarimetry of comet P/Halley	54
6. Polarimetry of comet P/Halley: Properties of dust	74
7. Polarimetric observations of some interesting objects	99

# CHAPTER 1

## Introduction

### Section 1.1 A brief history of cometary science

Among the various objects in our solar system, comets had attracted the attention of the common people to a large extent over the centuries. For a long time the scholars were not sure whether the comets have a celestial origin or an atmospheric origin. Aristotle himself used to believe that the comets are manifestations of some atmospheric phenomena. The positional measurements of comets by Toscanelli (1397-1482), attempted distance measurements by Peurbach (1423-1461), the observations by Fracastoro (1483-15530) that the comet tail is always pointed away from the Sun and the distance measurements of the bright comet during 1577, by Tycho Brahe gave the initial break through towards a systematic and scientific cometary research work.

Sir Edmond Halley, using Newtonian mechanics, showed that the comets which had appeared in 1531, 1607, and 1682 are the one and the same with a period of about 75.5 years. He also predicted that the comet would return in 1758. As predicted, the comet did return in 1758, though Halley had passed away by then. Later, the comet was named after him. This comet has been traced backwards in time, by several investigators through orbit calculations. It appears that this comet has so far made thirty historically recorded appearances.

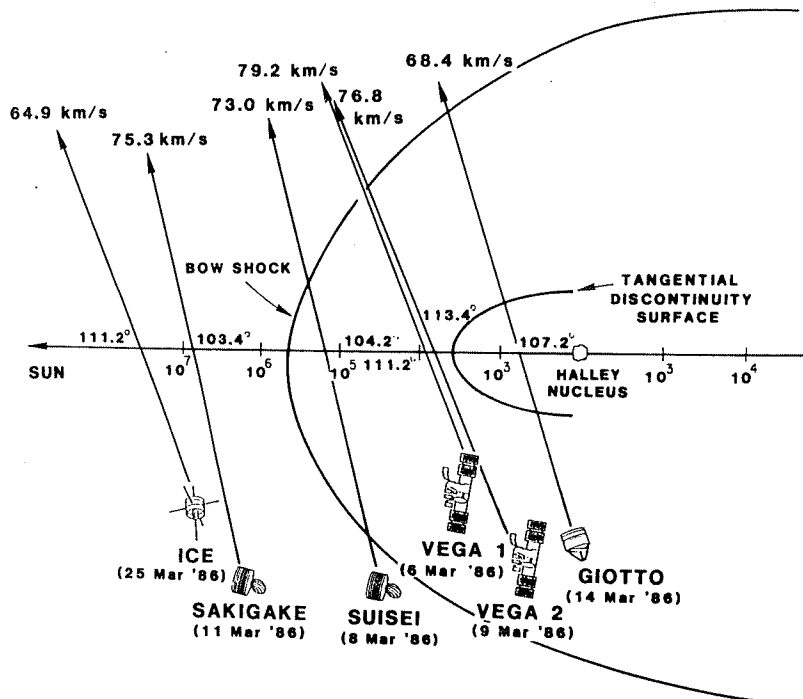


The successful predicted return of comet P/Halley, in eighteenth century, suggested that the comets are a part of the solar system moving in elliptical orbits. But later, as the physical appearances and the orbital characteristics of different comets were found to differ, Cole (1823) and others ruled out the periodicity in cometary orbits. It was suggested that the comets might come from the interstellar medium.

Johan Encke (1791-1864) discovered the non gravitational force by studying the cometary orbit of the famous comet (later named after him), with mathematical techniques developed by Gauss. He found that every 3.3 years, this comet returned 2.5 hrs earlier. It is now known that there are as well many comets returning later than the predicted period. This can be explained in terms of the outgassing from the surface of the comet. The outgassing from the afternoon side of the comet, results a non gravitational force due to the jet action, which adds to the rotation of the nucleus. If the rotation of the comet is in the same direction as the revolution around the Sun, then the outgassing will accelerate the revolution of the comet around the Sun, causing the decrease in the time period of the comet. In the reverse case the deceleration is caused.

## Section 1.2 The modern descriptions

Comets which contain both gas and dust, brighten up as they come closer to the Sun. At far distances from the Sun, it appears as a faint fuzzy patch of light, which is a cloud of gas and dust



Encounter speeds, dates, and geometries of the six spacecraft that flew by Comet

Figure 1. During March 1980, six spacecraft were sent by different nations to make insitu measurements on comet P/Halley.

called coma. In addition to the brightening of the coma, the tails start developing as the comet nears the Sun and approaches it's perihelion. After the perihelion the reverse process starts and the comet starts fading. The gas and dust in the coma, are released from a solid source (by solar heating), which is called the nucleus of the comet. The diameter of the nucleus can be a few kilometers. The diameter of the coma can be between  $10^4$  to  $10^5$  km. The nucleus and the coma form the head of the comet. The tail of the comet can extend up to  $10^7$  to  $10^8$  km.

#### Section 1.2.1 The nucleus

Before 1950, the nucleus of the comet was thought to be a collection of interstellar dust grains, attracted and captured by the gravity of the Sun, when the solar system passes through the galactic clouds in course of it's way around the galaxy. This model known as "Flying sand bank model" proposed by Lyttleton (1953) could not explain many of the observed phenomena in the comets.

The "dirty ice" model proposed by Whipple (1950) which describes the nucleus as a single aggregate of ices of water methane, carbon dioxide, ammonia etc and meteoritic matter, was able to explain various properties connected with cometary physics in a better way. However, the original model put forward by Whipple needs a number of improvements to understand (i) size of the nucleus (ii) its rotation period (iii) its internal structures etc.

The bare nucleus of a comet was actually seen, when comet

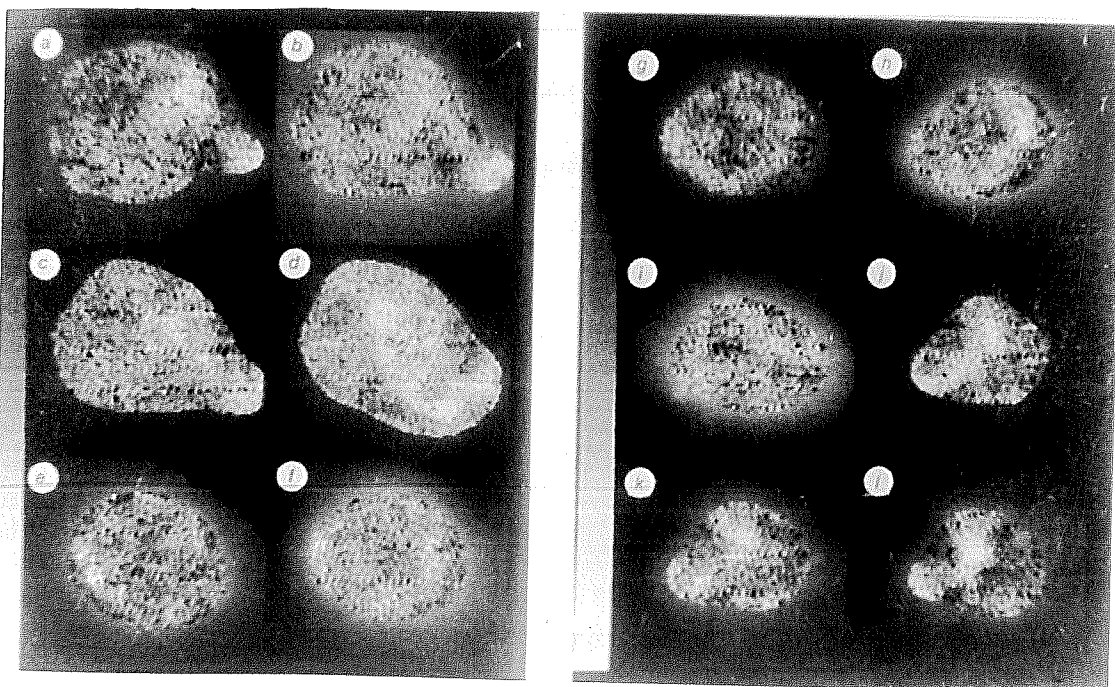


Figure 2. Processed images taken from Vega 1 on 6 March 1986, showing the nuclear region (Sagdeev et al. 1986a).

P/Halley was imaged by Vega and Giotto spacecrafts (Sagdeev et al. 1986a; Keller et al. 1986). Though this is the only comet for which a bare nucleus was actually seen, the existence of a cometary nucleus, as a single body, was predicted long before through the interpretations of several ground based observations. The nucleus of comet P/Halley was found to be an irregular potato shaped body  $\sim 14.0 \times 7.5 \times 7.5$  km in size, with a rotation period of  $53 \pm 3$  hrs (Sagdeev et al. 1986a). The albedo of the nucleus was found to be very low 0.04, probably this classifies P/Halley as the darkest object in our solar system (Sagdeev et al. 1986a). The temperature of the nuclear region was found to be 300-400 K by Vega (Sagdeev et al. 1986b)- which is much higher than that predicted by the ice models of nucleus (180-200 K, at the heliocentric distance of 0.8 AU). Sagdeev et al. (1986b) have suggested that the presence of a porous surface layer may be able to explain this anomaly. Several other physical parameters related with the nucleus of comet P/Halley have been determined during the recent apparition of the comet, which are not discussed here.

There are at present several modifications of the original 'dirty ice model' proposed by Whipple. But any model describing the cometary nucleus should be able to explain the above observed properties of the nucleus of P/Halley.

### Section 1.2.2 Cometary coma and tail

Various properties of the coma, like the size, gas and dust composition, production rates of different molecules, etc. depend upon the heliocentric distance of the comet, the composition of

volatiles in the outer layer of its nucleus and to a lesser extent on its rotation rate and polar axis alignment. By solar heating, the volatiles sublimate and drag with them the dust, flowing radially outward. The gaseous components emit the characteristic radiation in ultraviolet, visible, and IR wavelength due to several emission mechanisms. The simplest model for interpreting the gas emissions for comets is due to Haser(1957), which is discussed in chapter 3.

The photoionization of neutral molecules in the coma by solar ultraviolet radiation, produces ionic molecules (called cometary plasma) in the coma. The formation of an ion tail (also called Type I tail) is basically due to the interaction of solar wind plasma with cometary plasma. Interactions of this type was detected at a distance of  $\sim 1$  million km from the tiny nucleus by Suisei encounter of comet P/Halley (Kukai et al. 1986). The theoretical studies of the solar wind flow near the comet were carried out mainly in the framework of hydrodynamical description of plasma (Wallis 1973; Schmidt and Wegmann, 1982). The plasma tails are seen mainly due to the resonance fluorescence radiation from  $\text{CO}^+$  and  $\text{H}_2\text{O}^+$  molecules.

The dynamics of the dust particles released from the comet nucleus, depends upon the combined effect of solar radiation pressure and solar gravity and also on the size and mass of the particles. The dust particles are driven away from the nucleus by solar radiation pressure, forming a tail, called the dust tail (also Type II tail). This tail is seen due to the reflected solar continuum by the dust particles. The tail is curved so as to lag

behind the sun-comet line, opposite to the direction of cometary orbital motion. The particles with different size and mass follow different trajectories in the tail. The theory of dynamics of the dust tail is worked out in great detail by Finson and Probst (1968) and Sekanina and Miller (1973). Under favorable projection conditions, when the comet is close to the ecliptic plane the heavy dust particles, in the sunward direction of the comet appear as a tail pointing towards the Sun, called the anti tail.

### Section 1.2.3 Origin of comets

Oort (1950) showed that a simple plot of the number of comets versus  $1/a$ , the inverse of the semi major axis of the orbit, gave a conspicuous peak at around  $(1/a) \sim 10^{-5} (\text{AU})^{-1}$ . It was shown that, this peak can not be due to chance. Oort called the comets belonging to this peak as 'new' comets, which have come into the solar system for the first time. Most of these appear to come from a distance of  $\sim 10^5$  AU from the Sun. The inclinations of the orbits of these comets were found to be randomly distributed, similar to those of the observed long period comets. This appears to show the existence of a cloud of comets around the Sun at this distance, called the Oort cloud. Originally Oort made this plot with the data available on nineteen comets, but even now the data available on more number of comets continue to show the same trend.

According to the Oort theory there is a vast reservoir of comets around the Sun (called the Oort cloud), from which, due to the stellar perturbations, many comets leave the cloud for ever

and some others enter the planetary system. Among them some may happen to come close to Sun and are observable as new comets. A fraction of these comets, when encountered by the large planets (particularly Jupiter) are perturbed and leave the solar system all together after their first encounter. Some of them get caught in the solar system and seen as long period comets. By repeated encounter with giant planets many of them are transformed into intermediate period comets and finally into short period comets.

There are various hypotheses regarding the origin of Oort cloud. These can be broadly classified into two groups (i) the solar system origin and (ii) the interstellar origin. However, any scenario describing the origin of the comets must explain their dynamical properties as well as the chemical compositions. The presently known chemical compositions of comets require a temperature, at the time of formation, to be quite low  $\sim 80 - 200$  K to keep the volatiles like  $H_2O$  and  $CO_2$  from evaporating. This rules out the formation of comets in the inner solar system. The isotopic ratios of elements, like  $^{12}C/^{13}C$ , in the comet also put constraints in the temperature and age of the cloud, while modeling its origin.

### Section 1.3 The aims of the present work

Comet P/Halley made it's thirtieth historically recorded and fourth predicted return during 1985-86. Since comet P/Halley was one of the best predicted and intermediate period comet with its orbit known with a good accuracy, it was chosen as a target for six different space missions planned by the scientists all over



the world (Please see Figure 1). Simultaneously IHW (International Halley Watch organization) took up the responsibility of coordinating all the ground based observations made on comet P/Halley from different parts of the world.

The present thesis aims at understanding some of the physical parameters related with cometary dust, like its nature, size, composition and distribution. Since a large amount of cometary polarization is caused by the scattering of the sunlight by the cometary dust, these physical parameters can be studied effectively through photopolarimetric observations. The ground based photopolarimetric observations and the mass distribution functions of the cometary dust as obtained from the dust-mass detectors on board the spacecrafts, when analyzed together will be a powerful technique to explore different properties of the cometary dust. With these aims in mind, photometric and polarimetric observations were made on comet P/Halley in several continuum and emission bands. Also imaging polarimetry was carried out to study the spatial distribution of dust properties.

The cometary molecules produce a good amount of polarization by resonance fluorescence mechanism. But not much work has been done on the molecular band polarization of comets. One of the aims of the present thesis is to study the nature of molecular band polarization of a comet. Since it contaminates the observed continuum polarization, a proper understanding of the nature of the molecular band polarization will be useful (1) for carrying out accurate spectrophotometry of individual lines and (2) to calculate the actual polarization caused by the dust.

The distribution of dust is never homogeneous and smooth over the different regions of the comet. The combined effect of radiation pressure and solar gravity determines the path of a dust particle released from the comet nucleus. This distribution becomes further complicated when a dust jet is ejected from the nucleus. Imaging the entire comet in polarization would be, very useful to study the spatial distribution of the cometary dust and to probe the various nuclear activities.

The aims of the present thesis are:

- (i) to study the cometary molecular band emission and polarization
- (ii) to study the different properties of cometary dust
- (iii) to study the spatial distribution of cometary dust and probe for possible nuclear activities.

Apart from the above studies on comet P/Halley, the present thesis also describes some of the polarimetric studies taken up by the author on R Aquari and a set of supergiant stars.

## References

- Cole, W.: 1823, 'On the theory of comets', London
- Finson, M.L., and Probststein, R.F.: 1968, *Astrophys. J.*, 154, 327 (paper I), 353 (paper II).
- Haser, L.: 1957, *Bull Acad. Roy. Belg. cl. Sc.*, 5e Ser. 43, 740
- Keller, H.U., Arpigny, C., Barbieri, Bonnet, R.M., Cazes, S., Coradini, M., Cosmovici, C.B., Delamere, W.A., Huebner, W.F., Hughes, D.W., Jamar, C., Malaise, D., Reitsema, H.J., Schmidt, H.U., Schmidt, W.K.H., Seige, P., Whipple., F.L. and Wilhelm, K.: 1986, *Nature*, 321, 320.
- Kukai, T., Miyake, W., Terasawa, T., Kitayama, M., and Hirao, K., 1986, *Nature*, 321, 299.
- Lyttleton, R.A.: 1953, 'The comets and their origin', Cambridge University Press.
- Oort, J.: 1950, *Bull. Astr. Inst. Netherlands* 11, 91
- Sagdeev, R.Z., Szabo, F., Avanesov, G.A., Cruvellier, P., Szabo, L., Szego, K., Abergel, A., Balazs, A., Barinov, I.V., Bertaux, J.-L., Blamont, J., Detaille, M., Demarelis, E., Dul'nev, G.N., Endroczy, G., Gardos, M., Kanyo., M., Kostenko., V.I.,

S., Tarnopolsky, V.I., Toth, I., Tsukanova, G., Valnicek, B.I.,  
Varhalmi, L., Zaiko, Yu. K., Zatsepin, S.I., Ziman, Ya. L.,  
Zsenei, M., and Zhukov, B.S.: 1986a, Nature 321, 262.

Sagdeev, R.Z., Blamont, Z., Galeev, A.A., Moroz, V.I., Shapiro,  
V.D., Shevchenko, V.I., and Szego, K.: 1986b, Nature 321, 259

Schmidt, H.V., and Wegmann, R., 1982, 'Comets', edt L.L.  
Wilkening, University of Arizona press, p 538.

Sekanina, Z., and Miller, F.D.: 1973, Science 179, 565.

Wallis, M.K.: 1973, Planet. Space Sc. 21, 1647.

Whipple, F.: 1950, Astrophys. J., 111, 375

## C H A P T E R 2

### Instrumentation and observation

In this chapter the instruments used for the present observations are discussed along with the observational techniques. A two channel photoelectric photopolarimeter which works on rapid modulation principle was used for most of the observations made on comet P/Halley and other objects reported in this thesis. This instrument was mounted at the Cassegrain foci of one meter telescopes at Vainu Bappu Observatory, Kavalur and U. P. State Observatory, Nainital. In addition to this, we also carried out imaging polarimetry work of comet P/Halley using photographic technique on a Celestron-14" telescope at the Gurushikhar observatory, Mount Abu.

#### Section 2.1 Polarimetric definitions.

Before we go into the detailed description of the instruments, the definitions of different parameters, which are referred most frequently for any polarimetric work, are given below:

The most convenient way by which the polarization information can be described is through the four Stokes parameters (which are most commonly denoted by  $I$ ,  $Q$ ,  $U$ , and  $V$ ). These were first introduced by Stokes (1852). Recently Clarke(1974) defined  $I$ ,  $Q$ ,  $U$ , and  $V$  as discussed below:

The electric vector is used to describe the orientation of the electromagnetic wave vibration. A quasi monochromatic

electromagnetic disturbance may be written in terms of its components in the two orthogonal planes  $xz$  and  $yz$  as

$$E_x = E_{x0} \cdot \exp(i(\omega t - (2\pi z/\lambda) + \delta x)) \quad (1)$$

$$E_y = E_{y0} \cdot \exp(i(\omega t - (2\pi z/\lambda) + \delta y)) \quad (2)$$

where  $E_x$  and  $E_y$  are the values of the electric field vectors at the position  $z$  and at time  $t$ ;  $E_{x0}$  and  $E_{y0}$  are the amplitudes of the components of electric vector ( $E_0$ ) of vibration;  $\delta x$  and  $\delta y$  are the phases at  $z=0$  in the directions  $x$  and  $y$  respectively.  $\omega$  is the angular frequency and  $\lambda$  is the wavelength. For such a beam the Stokes parameters are defined as:

$$I = \langle E_{x0}^2 \rangle + \langle E_{y0}^2 \rangle \quad (3)$$

$$Q = \langle E_{x0}^2 \rangle - \langle E_{y0}^2 \rangle \quad (4)$$

$$U = \langle 2E_{x0} E_{y0} \cos(\delta y - \delta x) \rangle \quad (5)$$

$$V = \langle 2E_{x0} E_{y0} \sin(\delta y - \delta x) \rangle \quad (6)$$

The degree of polarization  $p$  is defined as

$$p = ((Q^2 + U^2 + V^2)^{1/2}) / I \quad (7)$$

Though these are supposed to be some of the most rigorous definitions of Stokes parameters, we shall use the definitions given by Serkowski (1962), which are more appropriate for astronomical measurements and are different from the above definitions by sign convention only. Here we consider  $l$  and  $r$  the two mutually perpendicular vectors in a fixed plane perpendicular

to the direction of propagation of the light beam. The cross product  $\mathbf{r} \times \mathbf{l}$  represents the direction of propagation of light and  $\mathbf{l}$  is lying in the plane of meridian of equatorial coordinate system and directed towards the northern hemisphere. The components of electric vector ( $E$ ) in some fixed point of space, as a function of time is written as :

$$E_l = E_{l0} \sin (\omega t - \epsilon_l) \quad (8)$$

$$E_r = E_{r0} \sin (\omega t - \epsilon_r) \quad (9)$$

where  $\omega$  is the angular frequency and  $\epsilon_l$  and  $\epsilon_r$  are the phases.

It is clear from Eq. (8) and (9) that the end of the electric vector ( $E$ ) in general will outline an ellipse in the  $lr$  plane. As has been discussed by Serkowski(1962) we can introduce two more parameters  $\theta$  and  $\beta$ , where  $\theta$  (usually called the position angle of polarization) is the angle which the major axis of the ellipse makes with the  $l$ -direction and  $\tan(\beta)$  is the ratio of the minor axis to the major axis of the ellipse. The angle  $\theta$  here is counted in the opposite direction compared to that of angle  $\chi$  of Chandrasekhar (1950) and van de Hulst (1957); consequently the present Stokes parameter  $U$  differs by the sign as compared to the same defined by the above authors. This change has been made in accordance with the direction in which position angle is measured in astronomy.

The Stokes parameters can now be rewritten in the form of the following four equations (Chandrasekhar, 1950)

$$I = E_{l0}^2 + E_{r0}^2 = (Q^2 + U^2 + V^2)^{1/2} \quad (10)$$

$$Q = E_{l0}^2 - E_{r0}^2 = I \cos 2\beta \cos 2\theta \quad (11)$$

$$U = -2 E_{10} E_{r0} \cos(\epsilon_1 - \epsilon_r) = I \cos 2\beta \sin 2\theta \quad (12)$$

$$V = 2 E_{10} E_{r0} \sin(\epsilon_1 - \epsilon_r) = I \sin 2\beta \quad (13)$$

The Stokes parameter  $I$  is the intensity of the beam. If we choose another system of coordinates  $I$  and  $\beta$  remain the same, only  $\theta$  changes. Thus  $I$ ,  $Q^2 + U^2$ , and  $V$  remain invariant under the change of coordinate system.

Actual light is the superposition of many simple waves coming in very rapid succession. If there exist no correlations between the phase differences  $\epsilon_1 - \epsilon_r$  and the amplitude ratio  $E_{10}/E_{r0}$  for these simple waves, we are dealing with unpolarized natural light. Otherwise the light is in general partially elliptically polarized. The Stokes parameters describing the actual light are the sums of the corresponding Stokes parameters describing the simple waves. This additive property of Stokes parameters leads to the principle of optical equivalence which says 'It is impossible by any optical analysis to distinguish between two beams characterized by the same set of Stokes parameters'.

In general light can be regarded as partially elliptically polarized. Such light described by four Stokes parameters can be decomposed into two beams:

1. Natural or unpolarized light of intensity  $I - (Q^2 + U^2 + V^2)^{1/2}$ ; for this beam  $Q = U = V = 0$ .

2. Fully elliptically polarized light of intensity  $(Q^2 + U^2 + V^2)^{1/2}$

If the intensity of this beam is much smaller than that of first beam, the light may be decomposed into three beams, namely:

1. Natural light of intensity  $I - (Q^2 + U^2)^{1/2} - |V|$

2. Fully plane polarized light of intensity  $(Q^2 + U^2)^{1/2}$ , for



which  $V=0$

3. Fully circularly polarized light of intensity  $|V|$  for which  $Q = U = 0$ ;  $V > 0$  corresponds to right hand circular polarization and  $V < 0$  corresponds to left hand circular polarization.

The ratio

$$P = (Q^2 + U^2)^{1/2} / I \quad (14)$$

is defined as the degree of polarization (or degree of linear polarization) and

$$P_v = |V|/I \quad (15)$$

is defined as degree of circular polarization.

The normalized stokes parameters defined above can also be expressed as :

$$Q / I = P \cos 2\theta \quad (16)$$

$$U / I = P \sin 2\theta \quad (17)$$

which are useful to determine  $P$  and  $\theta$  from measured values of  $Q$  and  $U$ .

## Section 2.2 Polarimetric observations, sources of errors and their remedies.

Most of the astronomical objects exhibit small polarization and therefore the demand for high accuracy in the polarization measurements becomes essential. There can be several sources of errors in polarimetric observations and some of them can be reduced quite effectively. Serkowski has dealt with these problems very elaborately (Serkowski 1962, Serkowski 1974). We shall mention some of the various sources of errors encountered in polarimetric measurements and their remedies as discussed by Serkowski (1974).

### (1) Photon Noise

The mean error of each of the simultaneously determined normalized Stokes parameters  $Q/I$  and  $U/I$ , which describe the linear polarization is

$$\varepsilon(Q/I) = \varepsilon(U/I) = \sqrt{2/N} \quad (18)$$

where  $N$  is the total photons counted. Thus the only method to reduce the error resulting from photon statistics is to count more photons. To make the most efficient use of the light available, one should subdivide the light into various frequency bands and detect all of them, simultaneously, with high quantum efficiency detectors.

### (2) Atmospheric scintillation and seeing

The air is not birefringent, therefore atmospheric scintillation will be same for both the perpendicularly polarized components of light coming from an astronomical object. The ratio of two such orthogonal beams, emerging from say a Wollaston prism, will be free from the effect of atmospheric scintillation.

The atmospheric seeing ie, the fluctuations and spread of the direction from which light is coming, affects the ratio of the two orthogonal components, since the detector on which the image forms will have inhomogeneous sensitive surface. This problem, which can as well arise due to the imperfect guiding in the telescope, can largely be solved by the introduction of an achromatic high focal length Fabry lens, which accurately images the primary mirror of the telescope on the photo cathode of the detector.

The harmful effect of both atmospheric scintillation and seeing can be suppressed by a rapid modulation of the signal. Unpublished calculation done by A. T. Young, quoted by Serkowski (1974),

shows that the sinusoidal modulation with frequency  $f$  diminishes the error of the atmospheric origin in the amplitude of this modulation by a factor  $(f/f_c)^{5/6}$ , where  $f_c$  is a cut off frequency equal to

$$f_c = V_{\perp} / (\pi D) \quad (19)$$

$D$  is the telescope diameter and  $V_{\perp}$  is the speed at which the wind drags the shadow pattern past the telescope aperture. Assuming  $V_{\perp} = 3000$  cm/sec, the critical frequency of modulation should be  $\sim 10$  Hz for a 100 cm diameter telescope, below which the photometric errors caused by atmospheric scintillation and seeing are not diminished.

In the present case, the modulation of the polarized radiation is achieved by mechanically rotating a half wave retarder. If the half wave retarder is rotated with a frequency  $f$  the emerging beam will have a modulation frequency of  $4f$  (as will be discussed later).

### (3) Instrumental Polarization

Linear polarization by the mirrors of a Cassegrain telescope does not exceed 0.1% if special precautions, described by Thiessen and Broglia (1959) are taken into account, while aluminising the mirrors. However, in all the telescopes this care is not taken. The telescope and the photopolarimeter optics may introduce some polarization which is called the instrumental polarization. The instrumental polarization can be determined by observing the zero polarization standard stars and the final result can be corrected for this instrumental polarization. A list of zero polarization standard stars is available from Serkowski (1974).

Also it is important to eliminate the conversion from linear to

circular polarization, which is caused by the telescope optics. Such a conversion diminishes the actual amount of linear polarization. Avoiding filters, lenses and tilted mirrors in front of an analyzer can help to a certain extent to get rid of this problem. Use of a dielectric focal plane diaphragm is essential, as the metallic diaphragms introduce polarization due to reflections. These cares have been taken into account in the present instrument which is discussed in the following section.

### Section 2.3 Description of the photopolarimeter

The photopolarimeter, which was built here at PRL and which was used for the present work, has been described by Deshpande et al (1985). An optical layout of the system is given in Figure 1.

The photopolarimeter works on a rapid modulation principle, which is achieved by the rotation of a half wave retarder. As can be seen from Figure 1., the photopolarimeter consists of a rotating half wave retarder, a similar fixed half wave retarder, a set of filters, a neutral density filter, a wollaston prism, and a detecting system with online processor. Both the half wave retarders are superchromatic (Pancharatnam 1955) and the retardance does not deviate more than  $3^\circ$  from  $180^\circ$  in the entire spectral range of 3100Å to 11000Å. The first half wave retarder is rotated at a frequency of 10.41 Hz, which results in the modulation of the polarized component of the radiation at 41.64 Hz. This fast rotation is essential to minimize the atmospheric scintillation effect, as has been discussed earlier. The first half wave retarder in addition to changing the retardance also changes the position angle of the optic axis, which is wavelength

dependent. This effect is totally eliminated by the use of a second half wave retarder which is identical with the first one but is fixed. The filter slide is situated after the two half wave retarders, so that the narrow band interference filters can also be used without the introduction of any instrumental polarization. The neutral density filter is used for brighter objects, to protect the photomultiplier tubes from being damaged owing to excess photon flux. The beam is split using a wollaston prism analyzer. The wollaston prism has been chosen as it gives the best separation angle between the two beams (ordinary and extraordinary) and has a good transmission in the wavelength region from 3150Å to 8500Å. Both the beams are detected using a set of GaAs sensitized photomultiplier tubes. These tubes have a flat response from 3150Å to 8500Å. The tubes are cooled to dry ice temperature to achieve low dark counts and are used in photon counting mode. The signal is integrated using coherent integration technique. The entire instrument is controlled by a Z-80 based microprocessor (presently replaced by IBM PC-AT). The data are analyzed for Stokes parameters and the results are obtained on line.

### Section 2.3.1 Calculation of polarization and position angle

Let the polarization vector of the incident beam make an angle  $\phi$  with the optic axis of the rotating half wave retarder at a particular instant of time. Also let the polarization vector of the beam after emerging out from the rotating half wave retarder make an angle  $\psi$  with the optic axis of the fixed half wave retarder. Let the Mueller matrices representing the rotating half

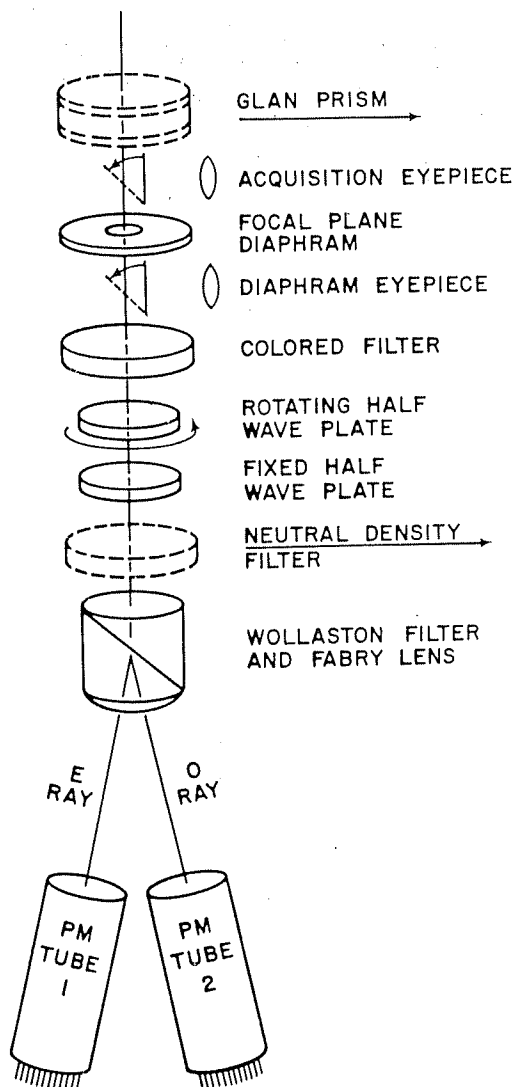


Figure 1. The optical layout of the photopolarimeter is shown.

wave retarder, fixed half wave retarder, and the wollaston prism be denoted by R, F, and W respectively. The expression for R, F, and W can be written as (Shurcliff 1962):

$$R = \begin{pmatrix} 1 & 0 & 0 & 0 \\ 0 & c2\phi & s2\phi & 0 \\ 0 & s2\phi & -c2\phi & 0 \\ 0 & 0 & 0 & -1 \end{pmatrix} \quad (20)$$

$$F = \begin{pmatrix} 1 & 0 & 0 & 0 \\ 0 & c2\psi & s2\psi & 0 \\ 0 & s2\psi & -c2\psi & 0 \\ 0 & 0 & 0 & -1 \end{pmatrix} \quad (21)$$

$$W = (1/2) \begin{pmatrix} 1 & \pm 1 & 0 & 0 \\ \pm 1 & 1 & 0 & 0 \\ 0 & 0 & 0 & 0 \\ 0 & 0 & 0 & 0 \end{pmatrix} \quad (22)$$

where  $c2\phi$ ,  $s2\phi$ ,  $c2\psi$ , and  $s2\psi$  stand for  $\cos 2\phi$ ,  $\sin 2\phi$ ,  $\cos 2\psi$ , and  $\sin 2\psi$  respectively. In the matrix expression (22) the upper sign stands for the ordinary and the lower sign for the extraordinary ray.

Let the Stokes parameters of the beam entering into the photopolarimeter be denoted by the matrix

$$\begin{pmatrix} I \\ Q \\ U \\ V \end{pmatrix}$$

Then one can obtain the Stokes parameters of the two light rays coming out of the wollaston prism as

$$\begin{pmatrix} I' \\ Q' \\ U' \\ V' \end{pmatrix} = W. F. R. \begin{pmatrix} I \\ Q \\ U \\ V \end{pmatrix} \quad (23)$$

A simple matrix multiplication utilising the expressions (20), (21), and (22) gives

$$\begin{pmatrix} I' \\ Q' \\ U' \\ V' \end{pmatrix} = (1/2) \begin{pmatrix} I \pm Q \cos 4\rho \pm U \sin 4\rho \\ Q \cos 4\rho \pm U \sin 4\rho \\ 0 \\ 0 \end{pmatrix} \quad (24)$$

where  $\rho = \phi - \psi$  = angle between the optic axis of the rotating and fixed half wave retarder. If  $\alpha$  and  $\beta$  are the position angle of the two half wave retarders, then from (22) we can write

$$I' = (1/2) [ I \pm Q \cos 4(\alpha-\beta) \pm U \sin 4(\alpha-\beta) ] \quad (25)$$

In the present case  $\alpha$  changes with frequency 10.41 Hz. Thus a complete rotation of the half wave retarder produces a modulation equivalent to four complete sine waves.

The half wave retarder rotates through 96 discrete positions by a stepper motor. Since one complete rotation produces data in one sine wave that is repeated in other 3 sine waves, data at similar phases are combined. Thus data collected from positions 1,25,49 and 73 are added. In a similar way data collected from positions 2,26,50 and 74 are added and so on. At each position the half wave retarder stops for 1 milli sec and samples the data.

When an integration is started an array of 24 locations in the computer memory is cleared. The counts obtained from combining of every twenty fourth position are stored into the memory and corrected for sky background. The number of photons counted by each photomultiplier tube is corrected for overlapping of pulses as discussed by Frecker and Serkowski (1974).

Let  $N_{ij}$  be the corrected number of photons for the position  $j$  of the half wave retarder ( $j = 1, \dots, 24$ ) and for the photomultiplier tube  $i$  ( $i = 1, 2$ ). Now from the relation (25) one can arrive at the



following equation for the photomultiplier tube  $i$  and position  $j$

$$Q_i \cos(15j) + U_i \sin(15j) = \pm (N_{ij} / \bar{N}_i - 1) \quad (26)$$

$$\text{where } \bar{N}_i = (1/24) \sum_{j=1}^{24} N_{ij}$$

the + sign is used for tube 1 and - sign for tube 2. There will be 24 such equations for each tube. The least square solution of above set of equations for each tube is

$$Q_i = \pm (1/12) \sum_{j=1}^{24} [ (N_{ij} / \bar{N}_i - 1) \cos(15j) ] \quad (27)$$

$$U_i = \pm (1/12) \sum_{j=1}^{24} [ (N_{ij} / \bar{N}_i - 1) \sin(15j) ] \quad (28)$$

The percent of linear polarization derived for each tube now can be written as

$$P = 100 (\pi/24) / \sin(\pi/24) \sqrt{Q_i^2 + U_i^2} \quad (29)$$

where  $100 (\pi/24) / \sin(\pi/24)$  is a factor correcting for the averaging of photon counts over 24 sections of sine curve (Frecker and Serkowski, 1970).

The error in  $P$  in percent can be derived as

$$\sigma_{P_i} = 100 \{ (1/22) [ (1/12) \sum_{j=1}^{24} (N_{ij} / \bar{N}_i - 1)^2 - (Q_i^2 + U_i^2) ] \}^{1/2} \quad (30)$$

(22 =  $n-2$ , where  $n = 24$  bins. One degree of freedom is lost in the averaging, another because of solving for two unknowns).

The expression for position angle also can be derived as:

$$\begin{aligned}
\theta &= \Delta\theta + 28^\circ.648 Z_i & \text{for } Q_i > 0, U_i > 0 \\
\theta &= \Delta\theta + 28^\circ.648 (Z_i + \pi) & \text{for } Q_i < 0 \\
\theta &= \Delta\theta + 28^\circ.648 (Z_i + 2\pi) & \text{for } Q_i > 0, U_i < 0
\end{aligned} \tag{31}$$

where  $\Delta\theta$  is the offset value in position angle to be determined after the observation of polarimetric standard stars and  $Z_i = \tan^{-1} (U_i / Q_i)$ .

The Q and U values combined for both the tubes can be expressed as:

$$Q = (1/12) \sum_{j=1}^{24} (R_j \cos(15j)) \tag{32}$$

$$U = (1/12) \sum_{j=1}^{24} (R_j \sin(15j)) \tag{33}$$

$$\text{where } R_j = (N_{1j} - N_{2j} (\bar{N}_1 / \bar{N}_2)) / (N_{1j} + N_{2j} (\bar{N}_1 / \bar{N}_2))$$

P,  $\theta$ , and  $\sigma$  now can be calculated from this set of Q and U values and by using relations (29), (30), and (31). The error in position angle can be expressed as follows (Serkowski, 1962):

$$\begin{aligned}
\sigma_\theta &= 28^\circ.65 \sigma_p / P & (\text{for } \sigma_p \ll P) \\
&= 51^\circ.96 & (\text{for } P \sim 0)
\end{aligned} \tag{34}$$

The expression for magnitude for the combined tubes can also be written as:

$$M = \Delta m - 1.08574 \ln ((\bar{N}_1 + \bar{N}_2) / 2t) \tag{35}$$

where  $t$  is the integration time and  $\Delta m$  is the offset value in the magnitude to be determined from the observations of photometric standard stars.

#### Section 2.4 Imaging polarimetry

Apart from the photopolarimeter described above, the comet P/Halley was observed in the imaging polarimetric mode also. The detailed description of the experimental set up used in the imaging polarimetry work will be separately discussed in chapter 5.

## REFERENCES

Chandrasekhar, S.: 1950, 'Radiative transfer' p 24. Oxford University Press (Clarendon), London and New York.

Clarke, D.: 1974, 'Planets, Stars and nebulae studied with photopolarimetry' p 45. ed. T. Gehrels, The University of Arizona Press.

Deshpande, M.R., Joshi, U.C., Kulshrestha, A.K., Banshidhar, Vadher, N.M., Mazumder, H.S., Pradhan, S.N., and Shah, C.R.: 1985, Bull. Astr. Soc. India 13, 157

Frecker, J.E. and Serkowski, K.: 1976 Appl. Optics. 15, 605

Pancharatnam, S.: 1955, Proc. Indian Acad. Sci A41, 137

Serkowski, K.: 1962, Advances in Astronomy and Astrophysics 1, 290.

Serkowski, K.: 1974, 'Planets, Stars and nebulae studied with photopolarimetry' p 135. ed. T. Gehrels, The University of Arizona Press.

Shurcliff, W.A.: 1962, 'Polarized light production and use' p 165, Harvard University Press, Cambridge, Massachusetts.

Stokes, G.G.: 1852, Trans. Camb. Philos. Soc. 9, 399

Thiessen, G., and Broglia, P.: 1959, Zeit. f. Astrophys. 48, 81

van de Hulst, H.C.: 1957, 'Light scattering by Small  
Particles.' p 42, Wiley, New York.

## CHAPTER 3

### Photometry of comet P/Halley

Cometary photometry is a very good tool for understanding the properties of cometary gas molecules as well as the dusts. The recent attempts by IHW (International Halley Watch) for coordinating all the ground based observations, by introducing a uniform set of filters, have helped us to make comparison between different sets of data supplied by different observers. In this chapter, the photometric observations taken on comet P/Halley, are presented and calculations are done for the emission flux values, column densities, and production rates of different cometary molecules.

#### Section 3.1 Observational details and reduction procedures

Observations were made on the one meter telescope of Vainu Bappu Observatory, Indian Institute of Astrophysics, Kavalur, India on 19 March 1986 with our photopolarimeter which gives online information on photometry and polarimetry. The comet coma was observed with 24" aperture (which corresponds to a linear size of about  $1.4 \times 10^4$  km). Another region across the dust tail (henceforth referred to as tail) was also observed with the same aperture, changing the RA and DEC each by  $-66''.6$  from the center of the coma (which corresponds to a distance of  $5.5 \times 10^4$  km).

IHW filter system was used for the observations, which contains

three continuum bands free from any cometary emissions: 3650/80, 4845/65 and 6840/90 and five emission bands CN(3871/50),  $C_3$ (4060/70),  $CO^+$ (4260/65),  $C_2$ (5140/90) and  $H_2O^+$  (7000/175) (all figures are in Angstrom, central wavelength/band pass). The extinction coefficients were obtained as the mean values of at least three standard stars chosen from those suggested by IHW organization. The solar type star HD105590 was observed for photometric calibration. This star has been chosen from a list of seven IHW solar analogs (given in IHW, Photometry and Polarimetry Net, Circular 8 Nov 1985). On the basis of the magnitudes of these solar analogs in 8 different IHW filters a set of interpolation formulae has been set up, which is given below (IHW Photometry and Polarimetry Net, Circular 3 Feb 1986):

We denote the magnitudes observed in the continuum filters 3650A, 4845A, and 6840A by  $m(3650)$ ,  $m(4845)$ , and  $m(6840)$  respectively. However, the magnitude observed in 4845A filter was corrected, for the neighboring  $C_2$  emission band (5140A) contamination, by the following empirical formula.

$$\text{corrected value of } m(4845) = m(4845) - 0.012 (m(5140) - m(4845))$$

This corrected magnitude is again denoted as  $m(4845)$  and following are the continuum magnitudes ( $m_c$ ) in the different emission filters :

$$m_c(3871) = 0.8151 m(3650) + 0.1849 m(4845) + 0.490$$

$$m_c(4060) = 0.6569 m(3650) + 0.3431 m(4845) + 0.088$$

$$m_c(4260) = 0.4895 m(3650) + 0.5105 m(4845) + 0.167$$

$$m_c(5140) = -0.2469 m(3650) + 1.2469 m(4845) + 0.244$$

$$\text{or} = 0.8521 m(4845) + 0.1479 m(6840) + 0.077$$

$$m_c(7000) = -0.0802 m(4845) + 1.0802 m(6840) + 0.039$$

.....(1a,b,c,d,e)

The above set of interpolation formulae was used to calculate the contribution of continuum in the emission bands in terms of the magnitudes. Since cometary emission is basically due to the scattering of the solar radiation, the expected spectrum of the comet is of solar type on which at certain wavelengths cometary emissions from CN, C<sub>3</sub>, CO<sup>+</sup>, C<sub>2</sub> and H<sub>2</sub>O<sup>+</sup> are superimposed (within the spectral range we are considering).

After necessary airmass corrections the observed magnitudes of the comet at different IHW filters are compared with the observed magnitudes of the solar type star HD105590 (the IHW standard magnitudes for this star are known); so that the former set of magnitudes are now reduced to the standard scale of IHW magnitudes. These magnitudes are converted into flux by adopting the flux conversion formulae given below ( IHW Photometry and Polarimetry Net, circular 3 Feb 1986):

$$F(\text{CN}) = (5.30 - 0.021 T) \times 10^{-7} \times (F(3871) - F_c(3871))$$

$$F(\text{C}_3) = (1.38 - 0.003 T) \times 10^{-7} \times (F(4060) - F_c(4060))$$

$$F(\text{CO}^+) = (5.90 - 0.005 T) \times 10^{-7} \times (F(4260) - F_c(4260))$$

$$F(\text{C}_2) = 6.81 \times 10^{-7} \times (F(5140) - F_c(5140))$$

$$F(\text{H}_2\text{O}^+) = 3.58 \times 10^{-7} \times (F(7000) - F_c(7000))$$

.....(2a,b,c,d,e)

where the unit is in erg-cm<sup>-2</sup>-s<sup>-1</sup> and T is the filter



Table 1. The observed magnitude ( $M_{\text{obs}}$ ), air mass corrected magnitude ( $M_{\text{cor}}$ ), and magnitude expressed in the IHW scale ( $M_{\text{IHW}}$ ) as discussed in the text are given along with the air mass values (AM) and coefficients of extinctions ( $K_{\lambda}$ ).  $F(\rho)$  gives the flux observed in the continuum ( $10^{-13}$  ergs-cm $^{-2}$ -s $^{-1}$ -A $^{-1}$ ) and emission ( $10^{-10}$  ergs-cm $^{-2}$ -s $^{-1}$ ) band. Other quantities  $\log M(\rho)$  and COMA/TAIL are as explained in the text.

$\lambda$	3650	3871	4060	4260	4845	5140	6840	7000
$K_{\lambda}$	.841	.649	.541	.451	.280	.227	.089	.027
HD105590								
AM	1.34	1.35	1.37	1.38	1.39	1.41	1.42	1.44
$M_{\text{obs}}$	10.80	11.29	9.28	9.24	8.47	8.52	9.62	8.95
$M_{\text{cor}}$	9.71	10.41	8.54	8.62	8.08	8.20	9.50	8.91
$M_{\text{IHW}}$	8.35	8.65	8.01	7.88	7.16	7.11	6.25	6.22
Comet (coma)								
AM	2.39	2.32	2.26	2.21	2.16	2.09	2.05	2.00
$M_{\text{obs}}$	13.50	11.42	10.61	11.33	10.36	9.06	11.19	10.43
$M_{\text{cor}}$	11.56	9.91	9.39	10.33	9.76	8.58	11.00	10.38
$M_{\text{IHW}}$	10.20	8.15	8.86	9.60	8.83	7.49	7.76	7.69
$F(\rho)$	6.86	2.36	2.42	0.07	14.72	4.75	13.03	0.06
$\log M(\rho)$		29.99	29.44	29.52		30.59		27.55
Comet (tail)								
AM	1.90	1.86	1.83	1.80	1.77	1.75	1.73	1.71
$M_{\text{obs}}$	13.65	11.36	11.29	12.16	11.29	9.72	12.33	11.56
$M_{\text{cor}}$	12.11	10.16	10.30	11.35	10.79	9.32	12.07	11.52
$M_{\text{IHW}}$	11.00	8.40	9.77	10.61	9.87	8.23	8.82	8.82
$F(\rho)$	3.28	1.99	1.02		5.67	2.68	4.88	
$\log M(\rho)$		29.92	29.07		30.34			
COMA/TAIL		1.19	2.36		1.77			

Table 2. Log of production rates ( $Q$  molecules- $s^{-1}$ ) of different molecules at the heliocentric distance  $r=0.99$  AU.

	CN	C <sub>3</sub>	C <sub>2</sub>
log $Q$	27.54	26.68	30.59

temperature in degree centigrade.  $F(\text{wavelength})$  is the magnitude converted into fluxes in arbitrary unit by the following formula

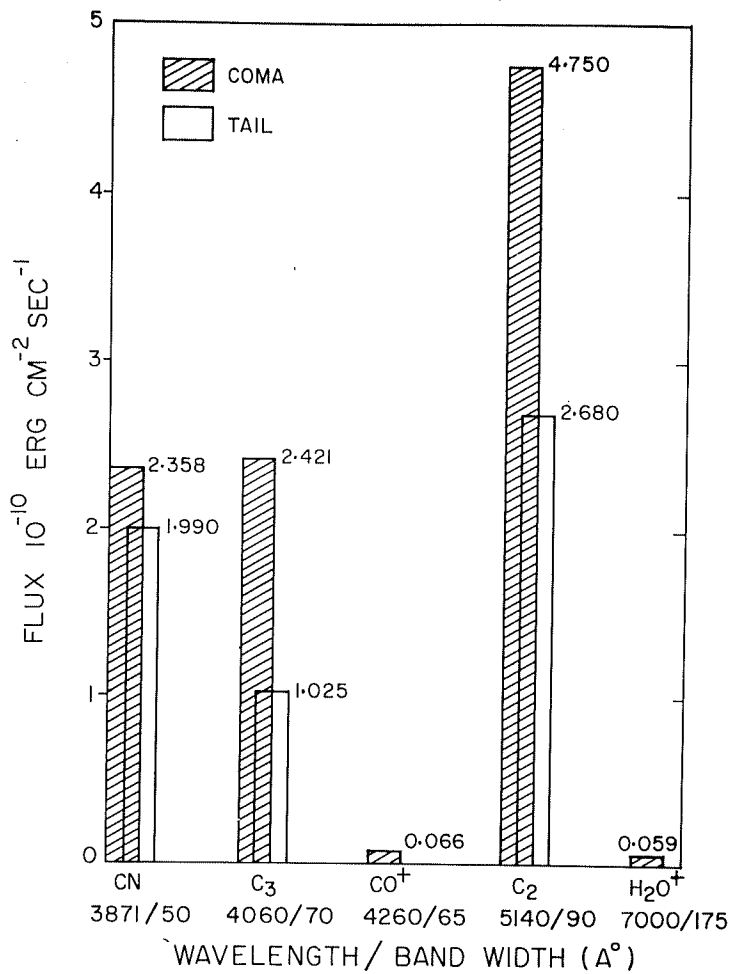
$$F(\text{wavelength}) = 10^{-0.4 m(\text{wavelength})}$$

The continuum fluxes ( $\text{erg-cm}^{-2}\text{-s}^{-1}\text{-\AA}^{-1}$ ) are determined from the following relations (IHW Photometry and Polarimetry Net, circular 3 Feb 1986) :

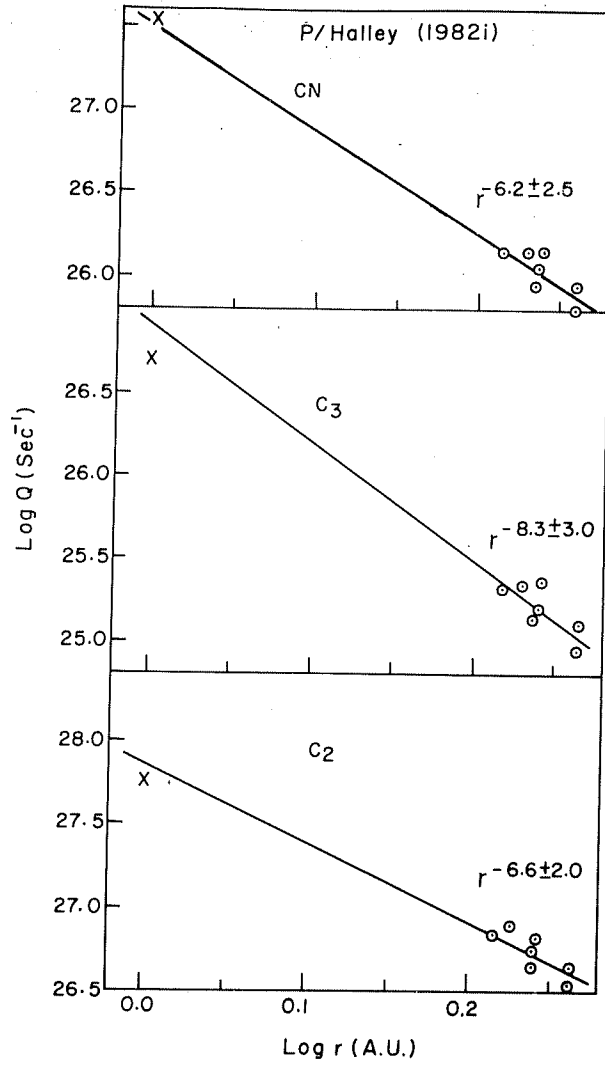
$$\begin{aligned} F_{\lambda} &= (8.22 \pm 0.13) \times 10^{-(9.0 + 0.4m(3650))} && \text{for } \lambda = 3650\text{\AA} \\ F_{\lambda} &= (5.10 \pm 0.30) \times 10^{-(9.0 + 0.4m(4845))} && \text{for } \lambda = 4845\text{\AA} \\ F_{\lambda} &= (1.65 \pm 0.02) \times 10^{-(9.0 + 0.4m(6840))} && \text{for } \lambda = 6840\text{\AA} \\ &&& \dots\dots\dots(3a,b,c) \end{aligned}$$

### Section 3.2 Discussions on the calculated flux values

In table 1 the extinction coefficients, air mass values and observed and airmass corrected magnitudes for the comet and solar type star HD105590 are given. Also fluxes in different emission bands ( $\text{CN}$ ,  $\text{C}_3$ ,  $\text{CO}^+$ ,  $\text{C}_2$  and  $\text{H}_2\text{O}^+$ ) for the coma and tail region, as discussed above are listed in Table 1. The calculated flux values have a maximum of 10% errors. Figure 1 shows histogram plots of these values. When considered in terms of total flux in the whole band one sees that  $\text{C}_2$  is stronger than  $\text{CN}$  and  $\text{C}_3$ , whereas  $\text{CN}$  and  $\text{C}_3$  are almost equal, for the coma region. Also for the coma region  $\text{CO}^+$  and  $\text{H}_2\text{O}^+$  fluxes are equal (within the error bar) and exhibit weaker emission compared to other emission bands. In the tail region (which will be at a distance of about  $5.5 \times 10^4$  km from the coma) the  $\text{CO}^+$  and  $\text{H}_2\text{O}^+$  emissions are below the detection limit.



1. Histogram plots of flux in different emission bands for coma and tail region.



2. Plot showing Log of production rates v/s Log of heliocentric distance taken from Catalano et al. (1987). The points marked by  $\odot$  represent observations by Catalano et al. (1987), whereas points marked by X represent our observations.

Table 1 also gives the flux ratio COMA/TAIL for different bands. Only CN,  $C_3$  and  $C_2$  have been considered for these ratios. It shows  $C_3$  is decreasing fastest along the tailward direction and  $C_2$  has decreased slightly faster than CN towards tail. This is expected, since  $C_3$  has smaller scale length (about  $4 \times 10^4$  km at 1.0 au) compared to CN and  $C_2$  (A'Hearn 1982; Delsemme 1975).  $C_3$  is generally found strongly concentrated in the nuclear region and has a larger slope than CN and  $C_2$  (Delsemme 1975). A faster decrease of  $C_2$  than CN can indicate a smaller scale length of  $C_2$  compared to CN. The spatial distribution study of CN by Combi and Delsemme (1980) shows CN has a scale length greater than  $3 \times 10^5$  km whereas the scale length of  $C_2$  is  $1.2 \times 10^5$  km (A'Hearn 1982); both the values being at 1.0 au. The intensity of  $CO^+$  and  $H_2O^+$  vary largely from comet to comet and little spectrophotometry has been done for them (A'Hearn 1982; Delsemme and Combi 1979).

### Section 3.3 Calculation of column densities and production rates

The number of molecules of each observed species, within a cylinder of radius  $\rho$  defined by the diaphragm and extending entirely through the coma can be evaluated by the standard formula (Millis et al., 1982):

$$\log M(\rho) = \log F(\rho) + 27.449 + 2 \log (\Delta \cdot r) - \log g \quad (4)$$

where  $F$  is the observed flux in cgs units;  $r$  and  $\Delta$  are the heliocentric and geocentric distances of the comet respectively and  $g$  is the fluorescence efficiency (in cgs unit) per molecule at  $r = 1$  AU. Following Millis et al. (1982) we use  $\log g(C_2) = -12.657$

and  $\log g(C_3) = -12.000$ . Because of Swings effect  $g(CN)$  varies significantly with comets heliocentric radial velocity. At the time of our observations the heliocentric radial velocity of the comet was 26.42 km/sec (IHW newsletter N 7). With this value of radial velocity, we have found out from the Figure 1 of Tatum and Gillespie (1977) that, the appropriate value of  $\log g(CN)$  is -12.360. From Babu et al. (1989) we take  $\log g(CO^+) = -13.441$  and  $\log g(H_2O^+) = -11.523$ . Now by using the relation (4) we calculate the value of  $\log M(\rho)$ , which have been listed in Table 1. Further by assuming the Haser model, the column densities ( $M(\rho)$ ) calculated for the coma can be converted into production rates for the neutral molecules by using the following relation (A'Hearn and Cowan, 1975)

$$M(\rho) = Q V^{-1} \rho \mu (\mu-1)^{-1} \left[ \int_x^{\mu x} K_0(y) dy + (1-1/\mu)/x + K_1(\mu x) - K_1(x) \right] \quad (5)$$

where  $V$  = velocity of the released species;  $\mu$  = ratio of daughter and parent molecule scale lengths;  $x$  = ratio of  $\rho$  and daughter molecule scale length;  $K_0$  and  $K_1$  are the modified Bessel functions of the second kind of order 0 and 1. We assume  $V = 0.58/\sqrt{r}$ , where  $r$  is the heliocentric distance of the comet (Delsemme, 1982; Cochran, 1985). We take the parent and daughter scale length values from Cochran (1985). The production rates for the neutral molecules  $CN$ ,  $C_3$  and  $C_2$  calculated by this method are listed in Table 2.

Catalano et al. (1986) have conducted the pre and post perihelion photometry of comet P/Halley for certain heliocentric distances. Our observations are at 0.99 AU heliocentric distance,

for which Catalano et al (1986) have no observations. They have plotted the  $\text{Log}(Q \text{ production rate})$  values across different  $\text{Log}(r)$  values for the molecules CN,  $C_3$  and  $C_2$ . They have found that  $Q \sim r^{-\alpha}$  where  $\alpha$  is  $6.2 \pm 2.5$ ,  $8.3 \pm 3.0$  and  $6.6 \pm 2.0$  for the molecules CN,  $C_3$  and  $C_2$  respectively. For a comparison, we have plotted the production rate values obtained by us on the same figure which is reproduced here as Figure 2. From this it is clear that within the errors, our production rate values follow the same trend of heliocentric distance dependence as obtained by Catalano et al (1986).



## References

- A'Hearn, M.F.: 1982, 'Comets' ed. L.L.Wilkening University of Arizona press, Tucson, Arizona, p 433.
- A'Hearn M.F., and Cowan J.J.: 1975, Astron. J. 218, 569
- Babu, G.S.D., Nathan, J.S., Rajamohan, R., and Sivaraman, K.R.: 1989, Bull. Astron. Soc. India, 17, 157
- Catalano, F.A., Baratta, G.A., and Strazzulla: 1987, Symposium on the Diversity and Similiarity of comets, 6-9 April 1987, Brussels, ESA SP-278, p 181
- Cochran A.L.: 1985, Astron. J. 90, 2609.
- Combi,M.R., and Delsemme, A.H.: 1980, Astrophys. J., 237, 641.
- Delsemme, A.H.: 1975, Icarus, 24, 95.
- Delsemm, A.H., and Combi,M.R.: 1979, Astrophys.J., 228, 330.
- Delsemme A.H.: 1982, 'Comets', ed. L. L. Wilkening, University of Arizona, Tuscon, USA, p 85
- Millis, R.L., A'Hearn, M.F., and Thompson, D.T.: 1982, Astron. J. 87, 1310

## CHAPTER 4

### Molecular band polarization of comet P/Halley

It is well known that cometary polarizations are caused by two mechanisms: (1) scattering of sunlight by the cometary particles and (2) fluorescence emission by the cometary molecules. However not much of work has been done towards the detection and measurement of molecular band polarization in comets. Ohman(1941) showed for the first time the presence of polarization due to resonance fluorescence emission. Further works are by Blackwell and Willstrop (1957), Bappu et al. (1967) and kharitonov and Rebristyi(1974). A recent work is by Le Borgne et al.(1987b), where they have measured for comet P/Halley and Hartley-Good, the resonance fluorescence polarization in the molecular bands of OH (3090 Å), CN (3880 Å) and C<sub>2</sub> (5140 Å).

#### Section 4.1 Observations and reduction procedures

Observations were made on the one meter telescope of Vainu Bappu Observatory, Indian Institute of Astrophysics, Kavalur, on 19 March 1986. The comet coma was observed with 24" aperture (which corresponds to a linear size of about  $1.4 \times 10^4$  km). Another region across the dust tail (henceforth tail) was also observed with the same aperture, changing the RA and DEC each by  $-66''.6$  from the center of the coma. The instrument used was a photopolarimeter which has been discussed in chapter 2.

IHW (International Halley Watch) filter system was used for our

observations, which contains three continuum bands free from any cometary emission: 3650/80, 4845/65 and 6840/90 and five emission bands: CN (3871/50),  $C_3$  (4060/70),  $CO^+$  (4260/65),  $C_2$  (5140/90), and  $H_2O^+$  (7000/175) (all figures are in Angstrom, central wavelength/ band pass ). The solar type star HD105590 was observed for photometric calibration. The entire photometric procedures, including how to obtain flux values in different emission bands, have already been described in chapter 3.

In the emission bands the observed flux is equal to the sum of flux due to reflected solar continuum(FC) and flux due to emissions from gas molecules(FE). The contribution of emission polarization to the observed polarization was found out with the help of Stokes parameters Q and U which have been already defined in chapter 2 and are as follows:

$$Q = P F \cos 2\theta \quad (1)$$

$$U = P F \sin 2\theta \quad (2)$$

where  $\theta$  = position angle and F = flux or intensity. The observed degree of polarization (PO) and position angle ( $\theta_0$ ) in emission bands are due to the mixing of emission with continuum. Thus by using Stokes parameters Q and U, one can estimate the emission polarization (PE) and position angle( $\theta_E$ ). The Stokes parameter due to observed polarization (QO, UO) is equal to the sum of the Stokes parameter due to emission polarization (QE, UE) and the Stokes parameter due to background continuum polarization (QC, UC). Therefore one can write

$$QO = QE + QC$$

$$UO = UE + UC$$

$$\text{OR} \quad PO \cos 2\theta O = PE \cos 2\theta E + PC \cos 2\theta C \quad (3)$$

$$PO \sin 2\theta O = PE \sin 2\theta E + PC \sin 2\theta C \quad (4)$$

where PC,  $\theta C$  and FC are the background continuum polarization, position angle and background continuum flux in the emission band. The degree of polarization and position angle in the continuum filters for coma and tail are listed in Table 1 (also Figure 1). From Figure 1 we find out, by interpolation, the degree of polarization in a particular emission band, which is due to background continuum only. In a similar way we find out the values of  $\theta C$  in different emission bands also. FE and FC values are calculated as discussed in chapter 3. The value of FO is simply the sum of FC and FE. After inserting the known values of FO, FC, FE, PO,  $\theta O$ , PC, and  $\theta C$  in the above set of two equations (3) and (4), we solve them for PE and  $\theta E$ . The results are listed in Table 2.

## Section 4.2 Results and discussion

The degree of polarization and position angle in the continuum filters for coma and tail region are listed in Table 1 (see also Figure 1). From our observations the position angle is found to be independent of wavelength and also perpendicular (within the errors) to the scattering plane. These features will be discussed in detail in chapter 6.

Fluxes in different emission bands (CN,  $C_3$ ,  $CO^+$ ,  $C_2$  and  $H_2O^+$ ) are given along with the background solar continuum flux in Table

Table 1 Percent polarization(P), error in polarization ( $E_p$ ) and position angle( $\theta$ ) in degrees in the three continuum filters for coma and tail.

		U Continuum	B Continuum	R Continuum
		3650/80	4845/65	6840/90
COMA	P	13.87	16.67	18.24
	$E_p$	1.35	0.21	0.46
	$\theta$	165	166	165
TAIL	P	9.38	14.29	18.99
	$E_p$	1.47	0.55	1.02
	0	164	167	171

2 for the coma and tail region. However, for the tail region the  $\text{CO}^+$  and  $\text{H}_2\text{O}^+$  emissions are below the detection limit. The molecular band polarization  $P(\beta)$  observed at a particular sun-comet-earth phase angle  $\beta$ , is supposed to follow the following theoretical relation (Ohman 1941)

$$P(\beta) = (P_{\max} \sin^2 \beta) / (1 + P_{\max} \cos^2 \beta) \quad (5)$$

where  $P_{\max}$  is the maximum polarization observed at a phase angle  $90^\circ$ . At the time of our observation the phase angle was  $66^\circ.1$ . Accordingly the  $P_{\max}$  values for the different molecules have been calculated and these values are listed in table 2.

From the theoretical calculations by Ohman (1941) a value of 7.7% for  $P_{\max}$  is expected for the molecules CN and  $\text{C}_2$ . The  $P_{\max}$  values obtained for CN and  $\text{C}_2$  in the present work seem to be well in agreement with the theoretically expected one (within the errors). Le Borgne et al (1987b) have found a very significant deviation of the CN polarization vector from the normal to scattering plane. But in the present work no such deviations were observed. In the present work, the  $\text{C}_3$  molecule shows a similar behavior to that of CN and  $\text{C}_2$ , with a  $P_{\max}$  value  $\sim 6\%$ . Le Borgne et al. (1987a) have reported a similar value for  $\text{C}_3$  band polarization, which is again much smaller than the theoretically expected value of 19%.

To have a first hand information about the errors which we are dealing with, while calculating polarization due to molecular emission, we proceed as follows:

The technique which has been discussed earlier to estimate the

Table 2		CN	C <sub>3</sub>	CO <sup>+</sup>	C <sub>2</sub>	H <sub>2</sub> O <sup>+</sup>
		3871/50	4060/70	4260/65	5140/90	7000/175
	PO	6.20	9.29	15.47	9.09	18.52
C	E <sub>po</sub>	0.43	0.29	0.45	0.14	0.29
O	θO	165	166	166	166	166
M	FC	0.326	1.697	0.781	2.129	2.958
A	FE	2.358	2.421	0.066	4.750	0.059
	PE	5.1	5.4	17.4	5.6	29.5
	θE	164	165	163	163	160
	P <sub>max</sub>	6.2	6.6	21.7	6.8	37.5
	PO	6.84	8.12	13.39	7.66	15.15
T	E <sub>po</sub>	0.53	0.55	0.83	0.28	0.83
A	θO	165	165	167	165	167
I	FC	0.150	0.754	0.335	0.796	1.106
L	FE	1.990	1.025		2.680	
	PE	6.5	5.3		5.0	
	θE	165	166		165	
	P <sub>max</sub>	7.9	6.4		6.0	

Note: PO=percent polarization observed in emission band; E<sub>po</sub>=error in PO; θO= position angle of polarization observed in emission band; FE=flux in emission band due to emission only and FC=flux in emission band due to background continuum only ( $10^{-10}$  ERG-CM<sup>-2</sup>-SEC<sup>-1</sup>); PE=emission polarization and θE=position angle of emission polarization estimated by using Stokes parameter; P<sub>max</sub>=max. pol. calculated from relation (5).

emission polarization becomes much simpler, if the emission and continuum have the polarization vector in the same direction (viz. perpendicular to the scattering plane). Such an assumption will not change our conclusion, as we have already seen the above assumption holds true, for our observations for the neutral molecules. In such a case the emission polarization PE is given by

$$PE \cdot FE = PO (FC + FE) - PC \cdot FC \quad (6)$$

where the observed polarization PO, is the vector sum of emission polarization (PE) and continuum polarization (PC). FC and FE are the flux due to background continuum and pure molecular emission respectively (as has been discussed already).

We shall use the relation (6) to estimate the errors associated with our calculated values of emission band polarization. Using the above relation (6) we can write ' $\delta PE$ ' the error in emission polarization in terms of the errors associated with the estimation of flux ( $\delta FE$  and  $\delta FC$ ). Thus

$$\delta PE^2 = \left( \frac{\partial PE}{\partial FC} \right)^2 \delta FC^2 + \left( \frac{\partial PE}{\partial FE} \right)^2 \delta FE^2 \quad (7)$$

At present we are not considering the error in the observed polarization value (PO) or in the continuum polarization value (PC). After partial differentiation we get from relation (7)

$$\delta PE^2 = \left( \frac{(PO-PC)}{FE} \right)^2 \delta FC^2 + r^2 \left( \frac{(PO-PC)}{FE} \right)^2 \delta FE^2 \quad (8)$$

where  $r = FC/FE$ .



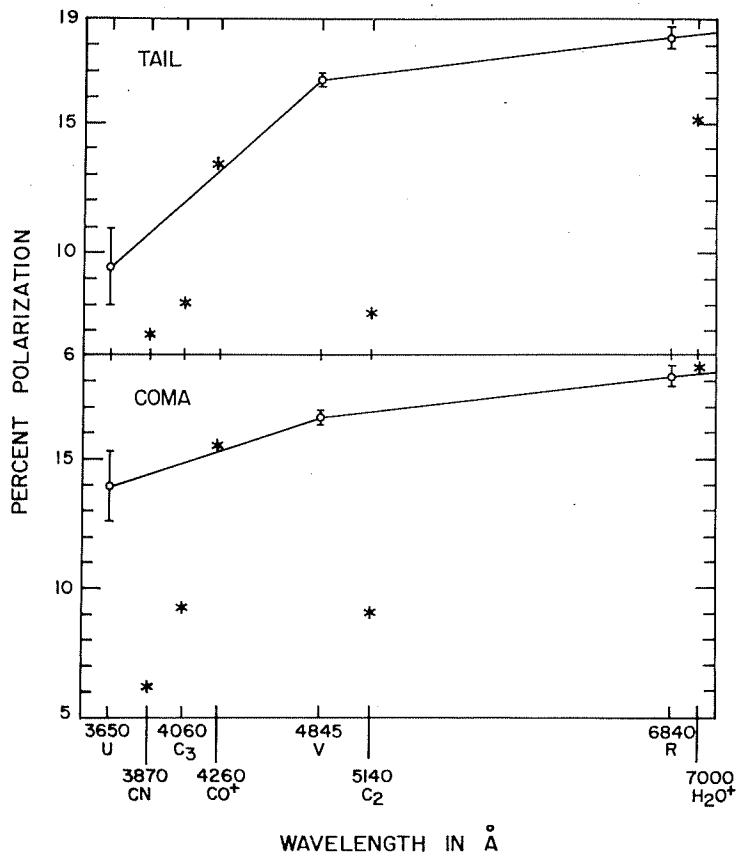


Figure 1. Wavelength dependence of linear polarization for coma and tail of comet P/Halley observed on 19 March 1986.

The calculated flux values in Table 2. has a maximum of 10% error. In the present case  $\delta FC$  and  $\delta FE$  are comparable and further if  $r \gg 1$ , (which is the case with  $CO^+$  and  $H_2O^+$ ) we can simply write

$$\delta PE \sim r ((PO-PC)/FE) \delta FE \quad (9)$$

Now we can clearly see from Table 2 that  $r > 10$  for the molecules  $CO^+$  and  $H_2O^+$ , which indicates that the values of the emission polarization derived by this method will have large errors. However, we see from the relation (8) that for the molecules  $CN$ ,  $C_3$  and  $C_2$  where  $r$  is always less than or close to 1,  $\delta PE$  also reduces.

In the present case both  $CO^+$  and  $H_2O^+$  show very high polarization values ( $P_{max} = 21.7\%$  and  $29.5\%$  respectively). Since the error bars associated with these values are very high, therefore it is difficult to make any definite conclusion about the nature of band polarization for these two molecules. However, one can argue that, if there is a large error present in the estimated emission polarization (PE) values, it may reflect on the estimated values of angle of polarization ( $\theta E$ ). But since the angles of polarization ( $\theta E$ ) estimated for  $CO^+$  and  $H_2O^+$  are same as that of all other molecules and continuum, we simply can not rule out the possibility of high polarization in the ionic bands.

Neither theoretical nor experimental works are probably available on the resonance band polarization of these two molecules. Further theoretical and experimental investigations are required for these molecules in future.

For all these molecular bands, the polarization vector was

found to be perpendicular to the scattering plane, which is generally expected.

The polarimetry of cometary molecular bands provides an useful test of the excitation conditions. It could be used at its best if, in the future, polarimetry of individual lines within a molecular band could be achieved. The anisotropy of fluorescence emission, which causes the band polarization, has generally being neglected in the construction of synthetic spectra. It could affect the line intensities by 10% or even more in extreme conditions (Le Borgne et al. 1987a). This effect should be taken into account when accurate comparison of theoretical and experimental spectra are made.

Since the presence of line emission contaminates the observed polarization which is due to dust, a proper understanding of the nature of molecular band polarization will help, in estimating the polarization which is purely due to the dust.

## References

Bappu, M.K.V., Sivaraman, K.R., Bhatnagar, A., and Natrajan, V.: 1967, Mon. Not. Roy. Astron. Soc., 136, 19

Blackwell, D.E., and Willstrop, R.V.: 1957, Mon. Not. Roy. Astron. Soc. 117, 590

Kharitinov, A.V., and Rebristyi, V.T.: 1974, Sov. Astron. 17, 672

Le Borgne, J.F., and Crovisier, J.: 1987a, Proc. of Symposium on the diversity and similarity of comets, Brussels, Belgium 6-9 April, 1987

Le Borgne, J.F., Leroy, J.L., and Arnaud, J.: 1987b, Astron. Astrophys. 173, 180

Ohman, Y. 1941. Stock. Obs. Ann., Band 13, no 11.

## CHAPTER 5

### Imaging polarimetry of comet P/Halley

During the recent apparition of comet P/Halley, linear and circular polarization measurements have been made by several investigators (Bastien et al., 1986; Brooke et al., 1987; Dollfus and Suchail, 1987; Kikuchi et al., 1987; Lamy et al., 1987; Le Borgne et al., 1987b; Metz and Haefner, 1987; Sen et al., 1988 etc). Most of these studies are aimed at understanding the polarization which occurs due to the reflection of the sunlight by cometary dust particles. These studies help us in understanding different properties of cometary grains. Polarization occurring due to the resonance fluorescence mechanism in the molecular emission bands of comet P/Halley has also been studied by some investigators (Le Borgne et al., 1987a; Sen et al., 1989). But most of these observations are taken through apertures, rather than imaging. Eaton et al. (1988) have carried out the imaging polarimetric studies in the near nucleus region of comet P/Halley on three different nights, showing the distribution of degree of polarization in different parts of the comet.

In order to study the degree of polarization and alignment of polarization vector within the different parts of the comet, we have carried out imaging polarimetry over an extended area of comet P/Halley.

In this chapter all the wavelength values are expressed in micron ( $\mu\text{m}$ ), in order to facilitate the comparison with the

similar works done by other authors in this field.

#### Section 4.1 Details of observation, and data reductions

Comet P/Halley was observed on 5 January, at 15-55 hrs. UT, ( $r=0.95$  AU and  $\Delta =1.24$  AU) with a 35 cm aperture f/11 telescope at Gurushikhar, Mt. Abu. The observation log has been given in Table 1. The images of the comet were obtained with an image intensifier placed at the focal plane and with a polaroid sheet placed in front of the primary mirror. Kodak 2415 film was used for photographic recording. The polaroid sheet, image intensifier, the photographic plate and the optics of the system together in combination had almost a flat response over the wavelength range of  $0.33 \mu\text{m}$  to  $0.68 \mu\text{m}$ , with a sharp cutoff in the longer wavelength side. Each exposure was of two minutes. Three photographs of the comet were taken in three different orientations ( $0^\circ, 120^\circ$  and  $240^\circ$ ) of the optic axis of the polaroid sheet with respect to the celestial N-S axis. If the intensities (corresponding to a particular point  $(x,y)$  in the comet image) in the three photographs are  $I_1$ ,  $I_2$  and  $I_3$  respectively then the polarization(P) and position angle of polarization vector( $\theta$ ), at the point  $(x, y)$  can be expressed as (Clarke, 1971)

$$P = \frac{2 * \sqrt{(I_1 (I_1 - I_2) + I_2 (I_2 - I_3) + I_3 (I_3 - I_1))}}{I_1 + I_2 + I_3} \quad (1)$$

$$\tan (2\theta) = \frac{\sqrt{3} * (I_3 - I_2)}{2I_1 - I_2 - I_3} \quad (2)$$

These three images were digitized with a photodensitometer system. After doing the photographic calibration, the intensity of light at each point of the image frame was found out. Later, with the help of image processing techniques and with the help of a field star SAO 145900 (towards the south east direction of nucleus) and the nucleus itself, the three frames were matched exactly. This field star is of K5 spectral type with visual magnitude 9.0. This star is not known to have any intrinsic polarization. In order to cover a wider field a transfer lens was introduced just before the image plane, which converts the beam into an f/8.7 one and gave a platescale of ~68 arc sec per mm. The field covered was 22 arc minute in diameter, centered on the nucleus on the photographic plate. As the geocentric distance of the comet was 1.24 AU, one arc sec in the image frame corresponds to about 900 km in the comet. One pixel on the image is  $60\mu\text{m} \sim 4$  arc sec  $\sim 3600$  km.

#### Section 4.1.1 Uncertainties in the estimated values of polarization:

An uncertainty  $\delta p$  in the measurement of polarization can be expressed in terms of the uncertainties in the measurements of intensities ( $\delta I_1$ ,  $\delta I_2$  and  $\delta I_3$ ) by the following relation

$$\delta p^2 = (\partial p / \partial I_1)^2 \delta I_1^2 + (\partial p / \partial I_2)^2 \delta I_2^2 + (\partial p / \partial I_3)^2 \delta I_3^2 \quad (3)$$

where  $\partial p / \partial I$  is the partial derivative of polarization  $p$  with respect to intensity  $I$ . Thus from relation (1) one can obtain :

$$\partial p / \partial I_1 = [ ( 2I_1 - I_2 - I_3 ) / (u v) ] - 2 u / v^2 \quad (4a)$$

$$\partial p / \partial I_2 = [ ( 2I_2 - I_1 - I_3 ) / (u v) ] - 2 u / v^2 \quad (4b)$$

$$\partial p / \partial I_3 = [ ( 2I_3 - I_1 - I_2 ) / (u v) ] - 2 u / v^2 \quad (4c)$$

where we have substituted

$$[ I_1 (I_1 - I_2) + I_2 (I_2 - I_3) + I_3 (I_3 - I_1) ]^{1/2} = u \quad (5a)$$

$$[I_1 + I_2 + I_3] = v \quad (5b)$$

combining (3), (4a), (4b) and (4c) we get

$$\begin{aligned} \delta p^2 &= (( 2I_1 - I_2 - I_3 )^2 \delta I_1^2 + (2I_2 - I_1 - I_3)^2 \delta I_2^2 + ( 2I_3 - I_1 - I_2 )^2 \delta I_3^2) / (u.v)^2 \\ &\quad + 4u^2 (\delta I_1^2 + \delta I_2^2 + \delta I_3^2) / v^4 \\ &\quad - 4(( 2I_1 - I_2 - I_3 ) \delta I_1^2 + (2I_2 - I_1 - I_3) \delta I_2^2 + ( 2I_3 - I_1 - I_2 ) \delta I_3^2) / v^3 \end{aligned} \quad (6)$$

Since  $\delta I_1$ ,  $\delta I_2$  and  $\delta I_3$  are comparable, we take  $\delta I_1 \sim \delta I_2 \sim \delta I_3 \sim \delta I$ , where  $\delta I$  is the average of the three uncertainties and thus the third term in expression (6) disappears. After necessary simplification we substitute back  $p=2u/v$  in (6) and we obtain

$$\delta p^2 = 6.\delta I^2/v^2 + 3 p^2 \delta I^2/v^2 \quad (7)$$

We further assume  $v = I_1 + I_2 + I_3 \sim 3I$ , where  $I$  is the average of the three intensities  $I_1$ ,  $I_2$  and  $I_3$ . Thus finally we get from relation (7)



$$\delta p \sim ((2+p^2)/3)^{1/2} (\delta I/I) \quad (8)$$

Since  $p$  is always smaller than 1 we simply write

$$\delta p \sim 0.82 (\delta I/I) \quad (8a)$$

All our intensity values are calculated from the linear portion of the photographic calibration curve, which is  $\text{Log}_{10} I = 0.454 + 2.833 D - 1.407 D^2$ , where  $D$  = photographic grain density. The above expression gives  $\delta I/I = 6.523 \delta D - 6.479 \delta D \cdot D$  and  $\delta I/I$  is maximum when  $D=0$ . Replacing  $\delta D$  by 0.001 which is the least count in the value of  $D$ , we get  $[\delta I/I]_{\text{max}} = 0.65\%$ . Thus the upper limit in the value of  $\delta p$  is 0.53%. However for most of the data points, which are brighter,  $\delta I/I$  is much smaller (typically  $\sim 0.2\%$ ).

Further the error in position angle can also be derived as

$$\delta \theta = \frac{(3 \cos^4 2\theta) ((I_2 - I_3)^2 \delta I_1^2 + (I_3 - I_1)^2 \delta I_2^2 + (I_1 - I_2)^2 \delta I_3^2)}{(2I_1 - I_2 - I_3)^4} \quad (9)$$

#### Section 4.1.2 Contamination from molecular emissions

The observed polarization (PO) in the present case will be a mixture of polarization (PC) due to dust scattering in the continuum and molecular band polarization (PE) in the emission. The observed polarization (PO) can be expressed in terms of PC and PE by using the Stokes parameters which are defined as follows.

$$Q = F P \cos 2\theta$$

$$U = F P \sin 2\theta \quad (10 \text{ a,b})$$

where F is the flux or intensity, P is the polarization and  $\theta$  is the position angle of polarization. The Stokes parameters are additive and one can directly write

$$Q_o = Q_c + Q_e$$

$$U_o = U_c + U_e \quad (11 \text{ a,b})$$

where the subscripts o,c, and e represent the quantities due to observed, continuum and emission polarization respectively. A detailed discussion showing how to separate these two components is given in chapter 4, where it has been shown that the position angle values for continuum and emission polarization are same. Under such circumstances the polarization (PO) observed within the wavelength range from 0.33  $\mu\text{m}$  to 0.68  $\mu\text{m}$  can be written as

$$PO = \sum_{\lambda=.33}^{.68} \frac{FC \cdot PC + FE \cdot PE}{FC + FE} \quad (12)$$

FC and FE being the flux values in the continuum and in the molecular emission respectively. In general FC, FE, PC and PE are all functions of wavelength  $\lambda$ . From the nature of the phase angle dependence of molecular band polarization (Le Borgne et al. 1987a and Sen et al. 1989) we assume an average value of 4% polarization for the three cometary molecules CN,  $C_3$  and  $C_2$  at  $51^\circ.5$  phase angle (as on 5 Jan 1986). For all other molecules

emitting within the above wavelength range, their contamination effect into the observed polarization will be negligible, since for them the product FE PE will be small as compared to the other three molecules. Also the wavelength dependence of continuum polarization for comet P/Halley was not very strong especially at small phase angles (Dollfus and Suchail, 1987; Brooke et al. 1987). Thus we can finally write without loosing much accuracy:

$$PO = PC \frac{\sum FC}{\sum FC + \sum FE} + PE \frac{\sum FE}{\sum FC + \sum FE}$$

$$= PC \, r / (r+1) + PE / (r+1) \quad (13)$$

$$= PC \, r / (r+1) + 0.04 / (r+1) \quad (13a)$$

where  $r = \sum FC / \sum FE$ . From Sivaraman et al (1987) we adopt a value of  $r = 3.71$  (corresponding to a date closest to and having same heliocentric distance as on, 5 Jan 1986). Their observations cover the wavelength range for the molecules  $C_3$  and  $C_2$  only and they also have suggested that inclusion of CN emission band will not change the value of  $r$  significantly. Under these assumptions relations (13) and (13a) reduce to:

$$PO = 0.788 \, PC + 0.212 \, PE \quad (14)$$

$$PO = 0.788 \, PC + 0.008 \quad (14a)$$

## Section 6.2 Discussion of results

Figure 1 shows one of the three photographs of the comet corresponding to the  $0^\circ$  orientation of the axis of the polaroid sheet with respect to celestial N-S, along with the intensity levels expressed in some arbitrary linear scale. The star SAO 145900 which has also appeared along with the comet image, can be

Table 1. Log of observations of comet P/Halley taken on 5 January 1986, from Gurushikhar, Mt. Abu, India. (  $r=0.95$  AU,  $\Delta=1.24$  AU, phase angle=  $51^\circ.5$ )

Frame No	Time in U.T when exposure started	Duration of each exposure	position of polaroid sheet w.r.t celestial north-south
1	15-55-32	2 minutes	$0^\circ$
2	15-57-40	-----	$120^\circ$
3	15-59-47	-----	$240^\circ$

easily seen in the south eastern side of the comet.

Figure 2 shows the distribution of degree of polarization in different parts of the comet. Background sky polarization is mixed up with actual cometary polarization over the entire image and from Figure 2, it appears to be generally between 0-2%. Since the comet was much brighter than the sky the error in measured polarization due to sky contamination will be much lower than 2%. We take an upper limit of 2% as an uncertainty in the estimated polarization values for the comet.

The star SAO 145900 seen in Figure 1, has disappeared from Figure 2. The position of the star SAO 145900 has been marked in Figure 2 by a white circle. The encircled region shows 0-2% polarization. Although the star should ideally show 0% polarization, but it will be always contaminated by background sky polarization which is between 0-2%. Thus with an accuracy of 2% polarization in our measurements we can claim that the star has disappeared from Figure 2. signifying that it is an unpolarized star. In fact the disappearance of this zero polarization star from Figure 2., acts as a calibration for our technique of imaging polarimetry and also confirms it.

Three distinct features are seen from Figure 2, (1) a region in the inner coma towards south west of the nucleus, having very little polarization (about 2%) (2) a region of very high polarization (about 10%) is seen almost at a distance of  $3.2 \times 10^5$  km from the nucleus in the tailward direction and (3) another region of relatively high polarization ( about 8%) is seen at about  $1.5 \times 10^5$  km from the nucleus also in the tailward direction. We refer these three regions as region 1, region 2 and region 3,

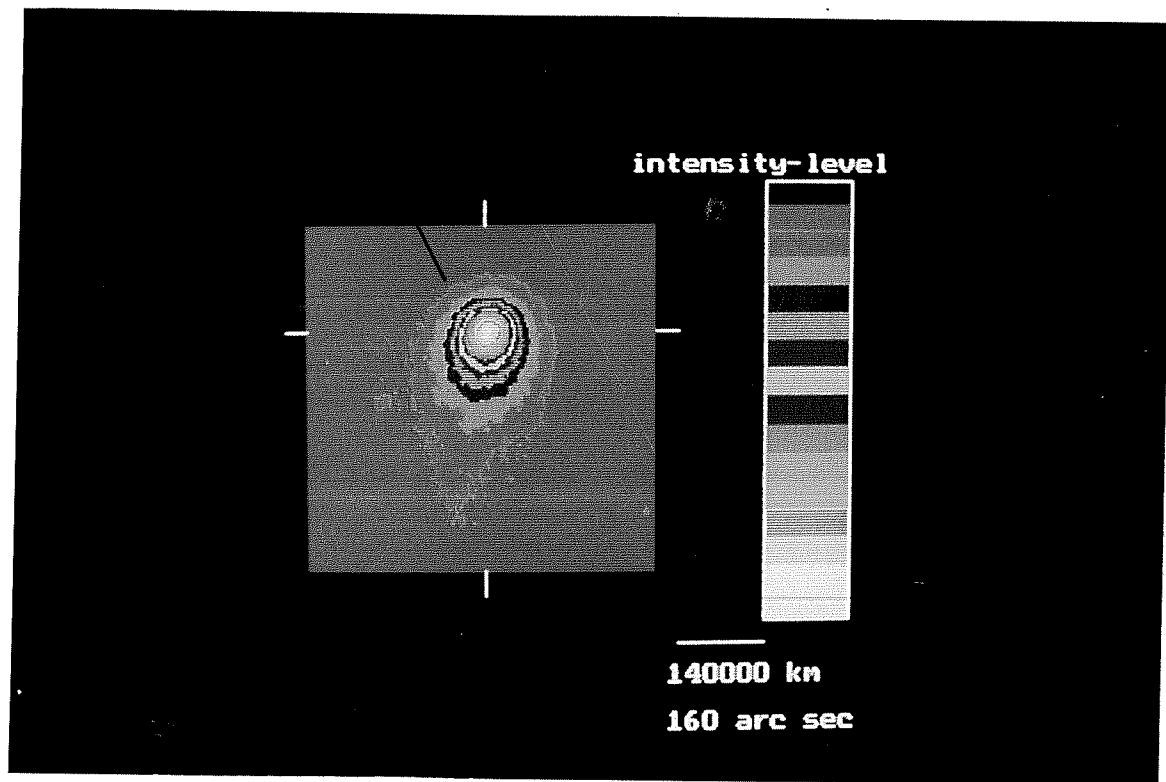


Figure 1.: Intensity image of comet P/Halley on 5 January 1986 is shown. Color coded intensity levels are expressed in some arbitrary linear scale. West is up and north is right in the photograph. Direction of sun is indicated by a tick mark, where a set of four small tick marks is used to identify the nucleus.

respectively in the subsequent discussion. The nucleus, as can be seen from Figure 2., itself has about 4% polarization.

Regions 2 and 3 can have high degree of polarization due to scattering, if the population of smaller grains is relatively higher in these regions. Eaton et al. (1988), have also done the imaging polarimetry of comet P/Halley on 5 January, 1986, at 16-50 UT, 55 minutes after our observations. They have also observed a similar region of high polarization, but at a much closer distance to the nucleus. The observed high polarization region as they have explained, can be due to several mechanisms. Apart from a high concentration of smaller size particles in these regions, grains with different values of refractive indices or a lower value of gas to dust ratio in these regions can explain the observed high polarization. Grains, after they are released from the nucleus, may change their optical properties (like refractive indices) with time due to evaporation of volatiles. Also grains which are originally released from the nucleus, will break up into small pieces as they move along the tail. Again since the observed polarization has contribution from the cometary molecular emission and molecular emission polarization is generally low compared to the dust component, a reduction in gas to dust ratio can also increase the observed polarization in a particular region. Also when a dust jet is ejected from the nucleus, the smaller size particles travel further, away from the nucleus compared to the large size particles, owing to their stronger coupling with the gas outflow and also due to more effective radiation pressure. The dust size distribution has been found from Vega and Giotto spacecraft, to be very complex and different for different parts

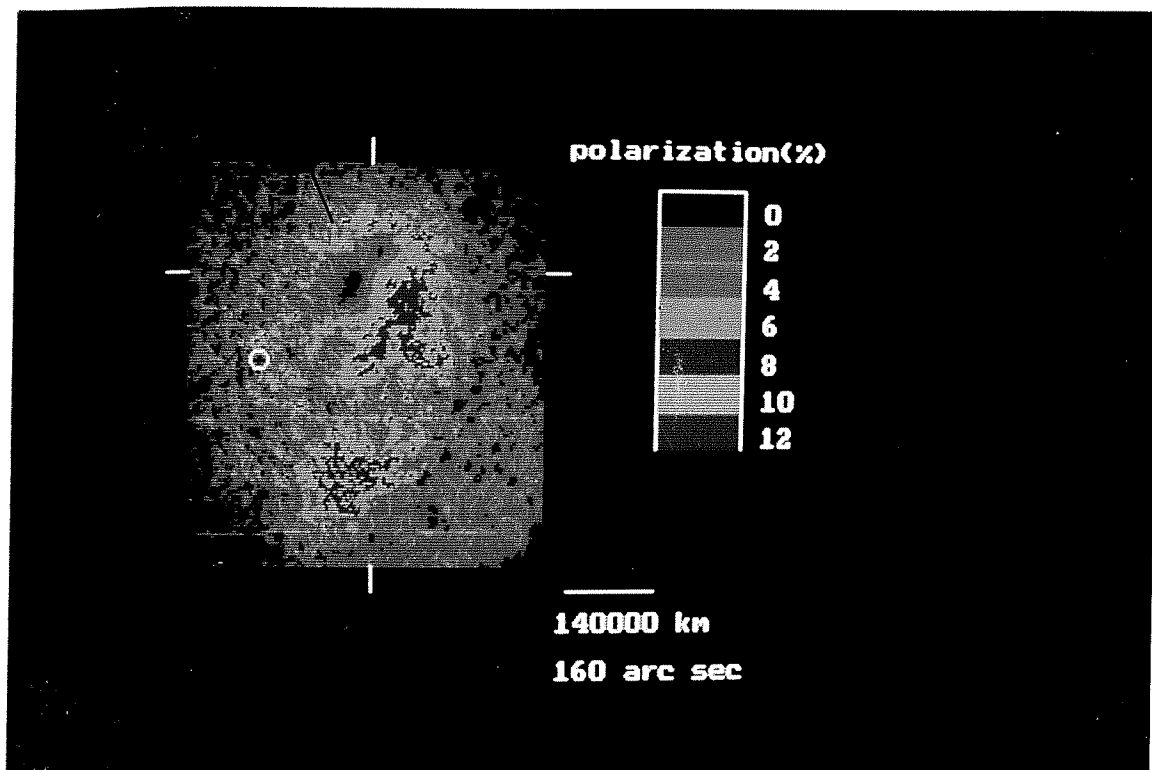


Figure 2.: Polarization image of comet P/Halley on 5 January 1986 is shown. Color coded polarization levels are shown alongside. West is up and north is right in the photograph. Direction of sun is indicated by a tick mark, where a set of four small tick marks is used to identify the nucleus. The position of the field star which was appearing in Figure 1 has been marked here with a white circle.



of the comet ( Mazets et al., 1987; McDonnell et al., 1986 etc). Dollfus and Suchail (1987) have studied polarizations of different parts of the comet, through ground based aperture measurements and found significant changes in polarization with nucleocentric distance.

In the following we make an attempt to evaluate the most likely mechanism from those suggested by Eaton et al. (1988) in explaining the high polarization blobs.

Apart from the regions 1, 2 and 3 the comet coma in general shows around 6% polarization and if we assume a value of  $r$  to be 3.71 there, then from (14a) we get a continuum polarization (PC) value of 6.5%. Therefore by changing the dust to gas ratio (which is related with  $r$ ) in the regions of high polarization blobs, we can at most raise the observed polarization ( $P_0$ ) value to 6.5%, but not to the extent of 8-10%, which is the observed degree of polarization in the blobs. Moreover by increasing the dust to gas ratio one can explain the high polarization blobs provided it is not done by reducing the amount of gas present there. The depletion of gas will show up in terms of lowering of intensity in the position of two blobs in Figure.1., which is not seen. Therefore more number of dust particles in the regions of these two blobs are required to explain the observations. These excess dust particles have to be sub-micron in size ( $\ll \lambda$ ), otherwise their existence will show up in the intensity map as the bigger particles ( $\geq \lambda$ ) have higher scattering efficiencies. Small grains ( $\ll \lambda$ ) will produce more polarization, but they will have less scattering efficiency compared to the bigger grains ( $\geq \lambda$ ) and as a result will have less effect on the intensity map. But simply

adding small grains sufficient to change the polarization would also affect the intensity. Therefore a change in the distribution of grain size which can result in the increase of the relative population of the smaller size grains is necessary, to explain the high polarization blobs. On the other hand if the grains change their optical properties by the evaporation of gases trapped in them, then they may be able to produce high polarization. But the change in optical properties are quite likely to change the scattering efficiencies as well, which should be seen on the intensity image. Therefore we suggest that concentration of smaller grains is the most likely mechanism, which can explain the high polarization blobs.

The origin of these two blobs (region 2 and 3) should be connected with the ejections of two discrete dust jets from the nucleus. Eaton et al. (1988) have covered a smaller field with higher resolution in their polarization images of the comet. Their observations were taken 55 minutes after our observations. Since dust jets are moving away from the nucleus, we can not see regions 2 and 3, in their polarization image as it covers a smaller field. But they also observed a high polarization region in the comet which seems to be around 14 arc sec from the nucleus, equivalent to 3.5 pixels in our image, which will be slightly difficult to identify. Therefore we can not comment about any connection between the high polarization blobs in the two sets of images. However, our observations cover much wider field (22 arc minute) compared to the field covered by Eaton et al. (1988) and both the sets of observations act as complementary to each other.

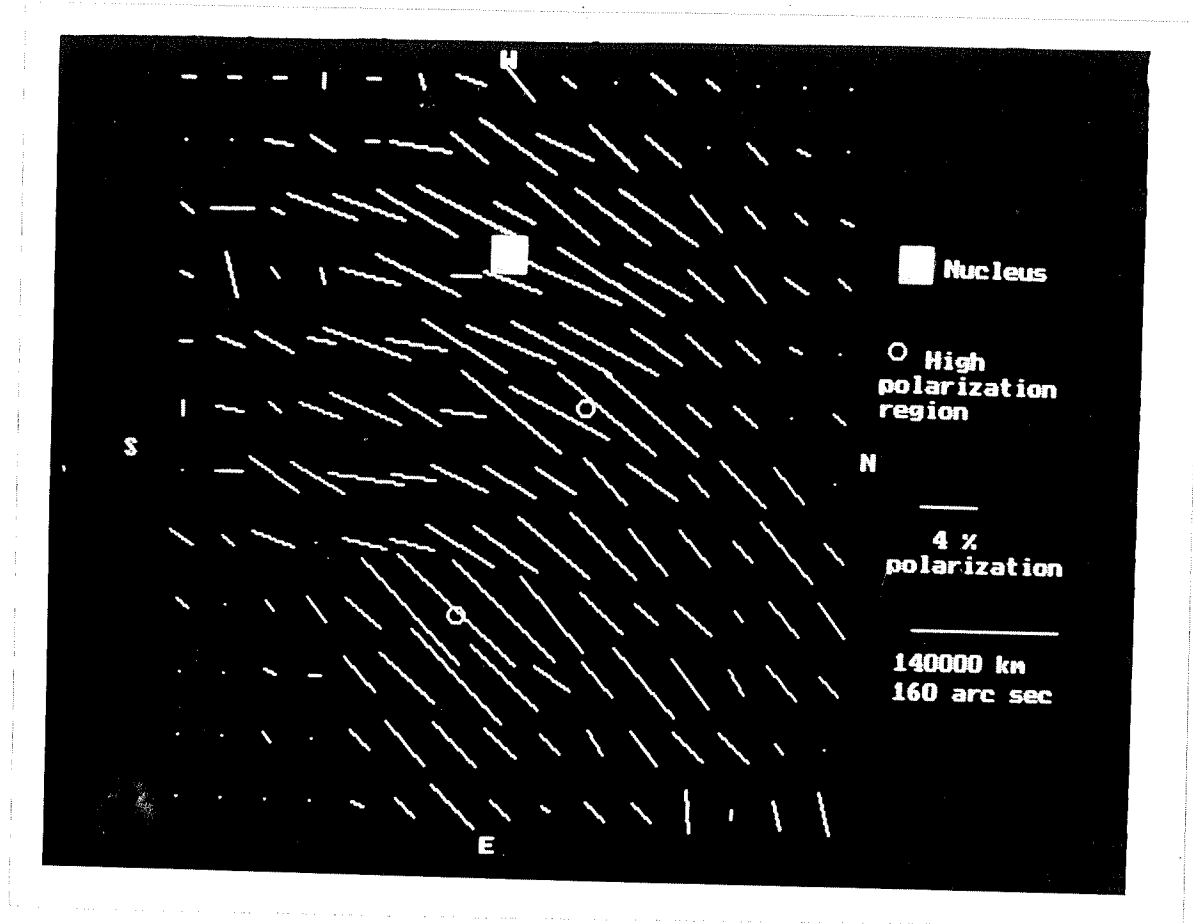


Figure 3.: The alignment of polarization vectors over different parts of the comet is shown. The degree of polarization is expressed in a suitable scale as shown along with. Position angle of each vector is measured from north towards east. In order to avoid the merging of two vectors which are almost parallel to the north south direction, we have added an angle of  $45^\circ$  to each of the actual position angle values of the polarization vectors. The nucleus, the two high polarization regions as discussed in the text and north south directions are marked.

### Section 6.2.1 A possible explanation for low polarization region

The existence of region 1, with very little polarization still remains to be explained. Apart from 5 January Eaton et al. (1988) have studied the comet on 13 December 1985 and 7 January 1986. Their 13 December polarization image shows, the nuclear region devoid of any polarization. Metz and Haefner (1987) from their circular polarization measurements suggest that multiple scattering was prevailing in the coma of comet P/Halley. Calculations by Keller et. al (1987) based on Giotto encounter of comet P/Halley suggest that the optical depth ( $\tau$ ) was less than 1.0. A value of  $\tau < 0.1$  is necessary for single scattering to take place, beyond this first double and then (for  $\tau > 0.3$ ) multiple scattering takes over ( Van de Hulst, 1981). One possible suggestion could be that the observed low polarization in region 1 may be caused by the depolarization due to multiple scattering. Comet Halley exhibited pronounced activities varying from night to night and occurrence of a dust jet can always raise the dust density to such an extent as to cause multiple scattering in some isolated regions in the coma.

Multiple scattering in general is possible in a region where the dust density is too high. But since in our case the region is not symmetric around the nucleus the question evidently arises whether it is connected with yet another fresh dust jet from the nucleus ? The observed low polarization in Region 1 probably can be connected with another fresh dust jet from the nucleus. A dust jet when it is ejected from the nucleus, can give high polarization by the already discussed mechanisms, only if the dust density is not too high to cause multiple scattering. Otherwise it

has to travel a sufficient distance from the nucleus until the dust density reduces to a value where the single scattering takes over the multiple scattering. Since the low polarization region is appearing like an arc around the nucleus we suggest, it was connected with an equatorial jet which was ejected continuously for quite sometime, so that due to the spinning of the nucleus it has taken the shape of an arc. Unfortunately the field coverage in the Eaton et al.(1988)'s photograph does not permit us to see this low polarization region in their photograph.

Figure 3 shows the distribution of polarization vectors over different parts of comet P/Halley. The degree of polarization is proportional to the length of the vector. The position angle of polarization vector is measured from north towards east. In the present case at some places the polarization vectors lie almost parallel to the north south direction and thereby two adjacent vectors merge together. In order to get rid of this difficulty we have added an angle of  $45^{\circ}$  to each position angle value in Figure 3. However, the direction of north south has been kept actual in Figure 3. It has been found that the polarization observed is positive, in other words, the polarization vector is perpendicular to the plane of scattering. No significant deviation from this trend is noticed for any part of the comet. It has been confirmed through several ground based aperture measurements that, except at small phase angles ( $<22^{\circ}$ ) the polarization observed for comet P/Halley is always positive ( see Kikuchi et al. (1987) and references therein). Our observations confirm this feature in a wider way, over the various parts of the comet P/Halley.

## References

- Bastien, P., Menard, F., and Nadeau, R.: 1986, Monthly Notices Roy. Astron. Soc , 223, 827.
- Brooke, T.Y., Knacke, R.F., and Joyce, R.R.: 1987, Astron. Astrophys. 187 , 621.
- Clarke, D.: 1971, Astron. Astrophys. 14, 90.
- Dollfus, A., and Suchail J.L.: 1987, Astron. Astrophys 187, 669
- Eaton, N., Scarrot, S.M., and Warren-Smith R.F.: 1988, Icarus 76, 270.
- Keller, H. U., Delamere, W.A., Huebner, W.F., Reitsema, H.J., Schmidt, H.U., Whipple, F.L., Wilhelm, K., Curdt, W., Kramm, R., Thomas, N., Arpigny, C., Barbieri, C, Bonnet, R.M., Cazes, S., Coradiny, M., Cosmovici, C.B., Hughes, D.W., Jamar, C., Walaise, D., Schmidt, K., Schmidt, W.K.H., and Siege, P.:1987, Astron. Astrophys. 187, 807.
- Kikuchi, S., Mikami, Y., Mukai, T., Mukai, S., and Hough, J.H. : 1987, Astron. Astrophys. 187, 689.
- Lamy, P.L., Grun, E., and Perrin, J.M. : 1987, Astron. Astrophys. 187, 767.
- Le Borgne, J.F., Leroy, J.L., and Arnaud, J.: 1987a, Astron.

Astrophys. 173, 180.

Le Borgne, J.F., Leroy, J.L., and Arnaud, J. : 1987b, Astron. Astrophys. 187, 526.

Mazets, E.P., Sagdeev, R.Z., Aptekar, R.L., Golenetskii, S.V., Guryan, Yu.A., Dyachkov, A.V., Ilyinskii, V.N., Panov, V.N., Petrov, G.G., Savvin, A.V., Sokolov, I.A., Frederiks, D.D., Khavenson, N.G., Shapiro, V.D., and Shevchenko, V.I. : 1987, Astron. Astrophys. 187, 699.

McDonnell J.A.M., Alexander, W.M., Burton, W.M., Bussoletti, E. Clark, D.H., Grard, R.J.L., Grun, E., Hanner, M.S., Hughes., D.W., Igenbergs, E., Kuczera, H., Lindblad, B.A., Mandeville, J-C, Minafra, A., Schwehm, G.H., Sekanina, Z., Wallis, M.K., Zarnecki, J.C., Chakaveh, S.C., Evans, G.C., Firth, J.G., Littler, A.N., Massonne L., Olearczyk, R.E., Pankiewicz, G.S., Stevenson, T.J., and Turner, R.F.: 1986, Nature. 321, 338.

Metz, K., and Haefner R.: 1987, Astron. Astrophys. 187, 539.

Sen, A.K., Joshi, U.C., Deshpande, M.R., Kulshretha, A.K., Babu, G.S.D., and Shylaja, B.S.: 1988, Astron. Astrophys. 204, 317.

Sen, A.K., Joshi, U.C., and Deshpande, M.R. : 1989, Astron. Astrophys., 217, 307.

Sivaraman., K.R., Babu, G.S.D., Shylaja, B.S., and Rajmohan, R.:

1987, Astron. Astrophys., 187, 543.

van de Hulst, H.C.: 1981, 'Light Scattering by Small particles'. p 6, Dover Publications, Inc., New York



## CHAPTER 6

### Polarimetry of Comet P/Halley : Properties of dust

Cometary polarizations are generally caused by two mechanisms: (1) scattering of sunlight by the cometary particles and (2) fluorescence emission by the cometary molecules. Linear and circular polarization measurements have been made by several investigators during the recent apparition of comet P/Halley (1982i) (Bastien et al., 1986; Brooke et al., 1987; Dollfus and Suchail, 1987; Kikuchi et al., 1987; Lamy et al., 1987; Le Borgne et al., 1987b; Metz and Haefner, 1987; Sen et al., 1988 etc). Most of these studies are aimed at understanding the nature of the polarization which occurs due to the scattering of the sunlight by cometary dust particles. These studies help us in understanding characteristics of cometary grains. Polarization occurring due to the resonance fluorescence mechanism in the molecular emission bands of comet P/Halley has also been studied by some investigators (Le Borgne et al., 1987a; Sen et al., 1989). The observed value of cometary linear polarization, which is caused by single dust scattering is generally a function of (1) incident wavelength (2) cometary phase angle ( $=180^\circ - \text{scattering angle}$ ) (3) the geometrical shape and size of the dust particles and (4) the composition of dust particles in terms of complex values of its refractive index ( $n-ik$ ); where the real part represents the actual refractive index and the imaginary part represents the absorption co-efficient of the dust particle. Since cometary particles are irregularly shaped and at present there is

no scattering theory available for irregularly shaped particles, we can reasonably make the assumption that cometary particles are spherical in shape and use Mie scattering formulation to explain the observed polarization values for a comet.

In the present chapter we will attempt to study the characteristics of cometary grains based on polarimetric observations through IHW (International Halley Watch) and other continuum filters.

Like the previous chapter, in this chapter also, all the wavelength values are expressed in micron ( $\mu\text{m}$ ), in order to facilitate the comparison of the results with similar works done by other authors in this field.

## Section 6.1 Observations

Observations were made with the one meter telescope of the Vainu Bappu Observatory, Indian Institute of Astrophysics, Kavalur, on 9, 10 Dec 1985 and 14, 15, 17, 18 and 19 Mar 1986, covering both the pre and post perihelion passages of comet P/Halley. A photopolarimeter, described in chapter 2, was used at the Cassegrain focus of the telescope.

On the nights of 9, 10 Dec 1985 and 17, 18 and 19 Mar 1986, the observations were taken through the IHW (International Halley Watch) filter system which contains three continuum bands centered at 0.365, 0.484 and 0.684  $\mu\text{m}$ , with FWHM 0.008, 0.006 and 0.009  $\mu\text{m}$ , respectively. An entrance aperture of 60" diameter was used on 9 and 10 Dec 1985 and 24" diameter was used on 17, 18 and 19 Mar 1986. On 9 and 10 Dec the observations were taken at around UT 15-00 hrs. But the observations on 17, 18 and 19 Mar were taken

Table 1. Percent polarizations as observed during Mar 1986, through different narrow band non-IHW continuum filters.

Date	Aperture (")	Phase-angle (°)	Wavelength ( $\mu\text{m}$ )	Polarization (%)
14-15 Mar	15	64.3	0.342	16.8 $\pm$ 1.0
			0.442	18.7 $\pm$ 0.2
			0.526	19.5 $\pm$ 0.2
			0.575	19.0 $\pm$ 0.2
			0.641	20.6 $\pm$ 0.2
15-16 Mar	15	64.8	0.526	18.6 $\pm$ 0.4
	24		0.526	18.4 $\pm$ 0.2
	15		0.641	19.0 $\pm$ 0.5

Table 2 : Percent polarization as observed during Dec 1985  
and Mar 1986 through the three IHW continuum filters.

Date	Aperture (")	Phase-angle (°)	U 0.365 $\mu$ m	B 0.484 $\mu$ m	R 0.684 $\mu$ m
9 Dec	60	44.3	9.3 $\pm$ 4.5	8.3 $\pm$ 1.1	9.3 $\pm$ 1.1
10 Dec	60	45.7	10.0 $\pm$ 3.0	6.8 $\pm$ 0.8	10.0 $\pm$ 1.3
17-18 Mar	24	65.9	15.9 $\pm$ 0.6	17.6 $\pm$ 0.1	20.0 $\pm$ 0.3
18-19 Mar	24	66.1	14.5 $\pm$ 0.9	18.3 $\pm$ 0.3	19.1 $\pm$ 0.3
19-20 Mar	24	66.1	13.9 $\pm$ 1.3	16.7 $\pm$ 0.2	18.2 $\pm$ 0.4

after UT 23-30 hrs. and since the observations were continued for an hour these observing dates are actually overlap between two nights such as 17-18, 18-19 and 19-20 Mar respectively. However in the subsequent discussions (except in the Tables 1,2,3) we will refer these three nights as 17, 18 and 19 Mar for convenience. On the nights of 14 and 15 Mar 1986, the comet was observed through several other narrow band interference filters centered at 0.342, 0.442, 0.526, 0.575 and 0.641  $\mu\text{m}$ , all the filters have FWHM  $\sim$  0.005 $\mu\text{m}$ . These filters except 0.575  $\mu\text{m}$  (which is slightly contaminated by  $\text{NH}_2$  emission) are free from any cometary molecular emission. All the observations were centered around the nucleus and the diameter of the aperture was 15" and 24". As discussed above these two nights are also actually overlap between the two nights 14-15 and 15-16 Mar respectively. But in the subsequent discussion, except in Table 1, we will refer them as 14 and 15 Mar respectively. For these five overlapping nights we tabulate the phase angle values (in Table 1 and 2) which correspond to the phase angle at the UT 00.00 hrs of the second night. Also we shall use these values for Mie scattering calculations to be discussed later.

## Section 6.2 Results and Discussions

In Table 1 we have listed all the polarization observations taken through non-IHW continuum filters, which are plotted in Figure 1. From Figure 1 we can clearly see that the polarization increases with wavelength on 14 and 15 Mar. The observations on 14 Mar were made also with the filter 0.575  $\mu\text{m}$  which is slightly contaminated by  $\text{NH}_2$  emission. On 14 Mar all the observations were

Table 3. Percent polarizations observed through the non-IHW filters are compared here with the expected polarization values calculated, using n and k values estimated as discussed in the text.

Phase Angle (°)	Wavelength in $\mu\text{m}$	Observed Polarization (%)	Estimated values of (see text)		Expected Polarization (%)
			n	k	
64.3	0.342	16.8 $\pm$ 1.0	1.311	0.031	16.8
	0.442	18.7 $\pm$ 0.2	1.376	0.037	18.2
	0.526	19.5 $\pm$ 0.2	1.374	0.042	18.8
	0.641	20.6 $\pm$ 0.2	1.374	0.049	19.1
64.8	0.526	18.6 $\pm$ 0.4	1.374	0.042	19.0
		18.4 $\pm$ 0.4			19.0
	0.641	19.0 $\pm$ 0.5	1.374	0.049	19.3

Table 4. Percent polarization as expected at different scattering angles (in degrees) with particle size range 0.001-20.0 and 0.01-20.0  $\mu\text{m}$  respectively  $((n,k)=(1.387,0.032), \lambda=0.365\mu\text{m})$ .

Particle size range 0.001-20.0 $\mu\text{m}$ ,									
Scat. angle	100	110	120	130	140	150	160	170	180
Polarization	23.7	21.0	14.7	8.4	2.8	1.8	1.5	-4.4	0.0

Particle size range 0.01-20.0 $\mu\text{m}$ ,									
Scat. angle	100	110	120	130	140	150	160	170	180
Polarization	15.3	10.1	6.4	4.0	2.4	1.4	0.8	0.5	0.4

taken through the 15" aperture and we have joined these data points in Figure 1 by straight lines except the point corresponding to 0.575  $\mu\text{m}$ . Figure 1 shows that the polarization decreases across the band 0.575  $\mu\text{m}$ . This is quite expected, since the molecular emission is generally polarized to a lesser extent as compared to the continuum polarization caused by dust (Le Borgne et al., 1987a; Sen et al., 1989). On 15 Mar we have observed the comet only through two continuum filters 0.526 and 0.641  $\mu\text{m}$ , with 15" aperture. Here also we see an increase in polarization with wavelength. In order to see whether the polarization changes with the size of the entrance aperture, we have repeated the observation at 0.526  $\mu\text{m}$  with 24" aperture on the same night. However as seen from Figure 1. and Table 1. the polarization does not seem to change, within the errors, when we change the aperture size from 15" to 24". Bastien et al.(1986) have done similar studies and by changing the aperture from 3".9 to 17".7, they have found that barring some exceptions, there is a general trend for the polarization to decrease as the aperture size increases. Their experiments were conducted at wavelengths 0.764 and 0.684  $\mu\text{m}$ , over a range of phase angle from  $20^\circ$  to  $52^\circ$ . Bastien et al.(1986) have also discussed the cases of other comets where sometimes the opposite trend has been noticed. Kikuchi et al.(1987) have changed the aperture from 13" to 32".6, for comet P/Halley and found no systematic dependence of polarization on the aperture size.

In Table 2 we have listed all the observations taken through the IHW continuum filters and in Figure 2 we have plotted them. The observations taken on 18 and 19 Mar correspond to the largest



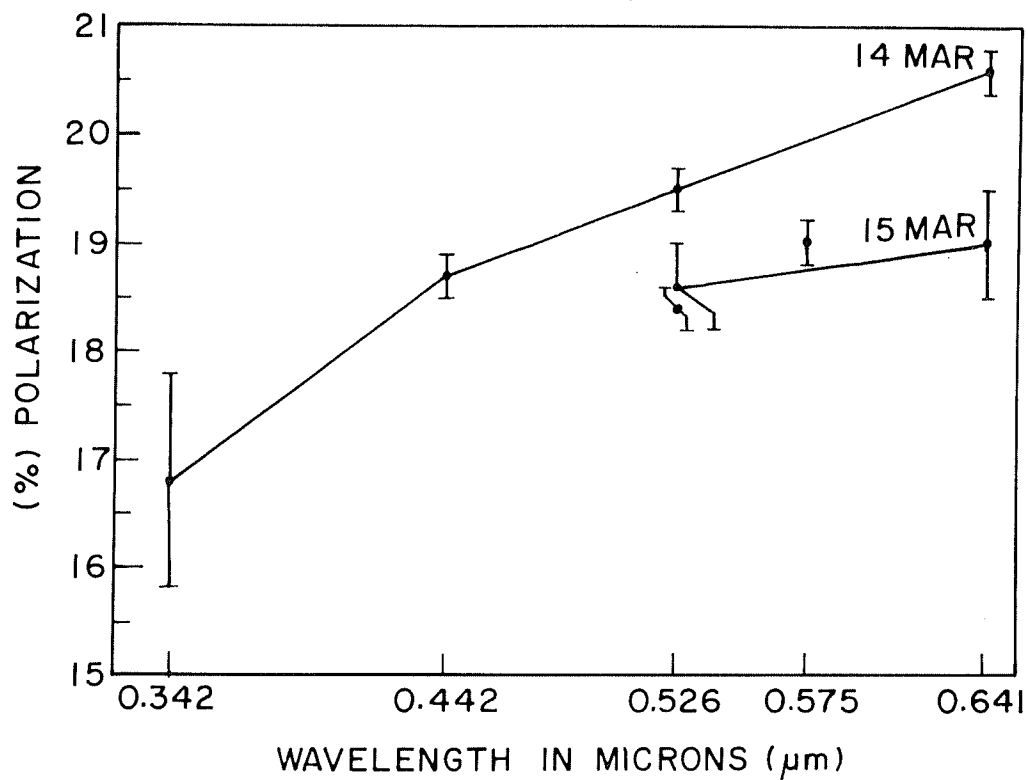


Figure 1. Wavelength dependence of polarization observed through several non-IHW continuum filters on 14 and 15 Mar 1986.

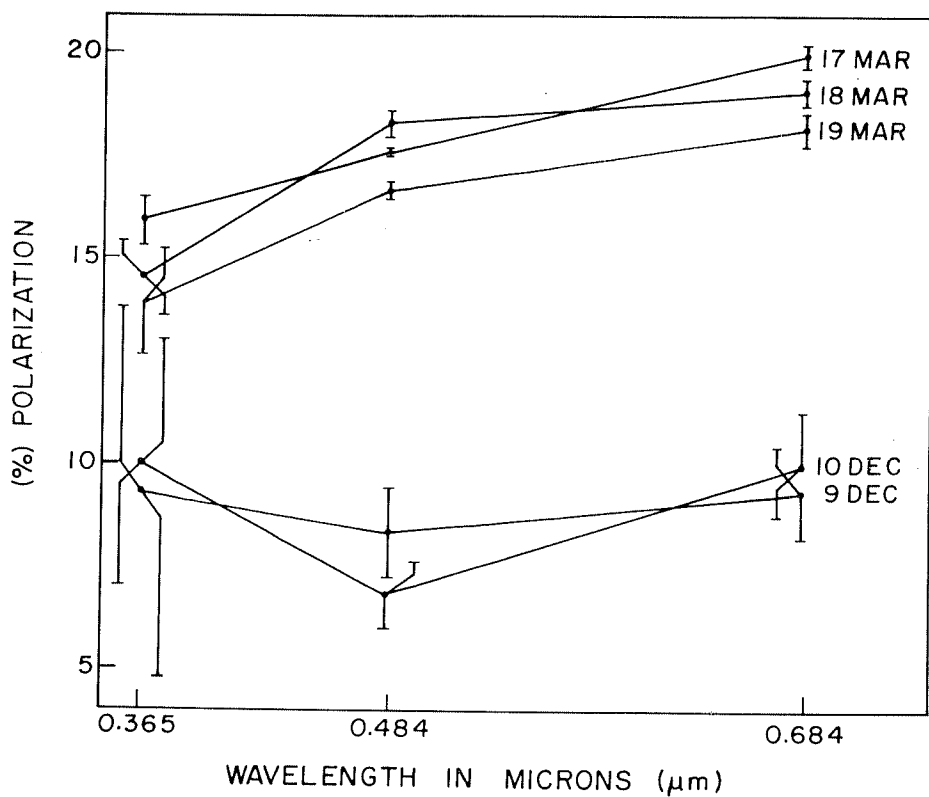


Figure 2. Wavelength dependence of polarization observed through three different IHW continuum filters during Dec 1985 and Mar 1986.

phase angle for which ground based observations were possible on comet P/Halley. As seen from Figure 2, the post perihelion polarization values increase with the wavelength, whereas for the pre perihelion observations no such trend is seen within the errors. In our case the post perihelion observations correspond to a phase angle  $\sim 66^{\circ}$ , whereas pre perihelion observations were made at a phase angle of  $\sim 45^{\circ}$ . As has been reported by other authors (Kikuchi et al., 1987; a more general review is given by Dollfus et al., 1988) comet P/Halley's polarization showed a clear increase with the wavelength for higher phase angle values, but no such dependence was seen for smaller phase angles. Brooke et al. (1987) confirmed this trend from their IR polarimetric observations also.

Bastien et al. (1986) have found that the polarization becomes negative (electric vector becomes parallel to the scattering plane) when the phase angle is  $\leq 22^{\circ}$ . The polarization observed in our case is always positive. In other words the direction of electric vector was always perpendicular to the scattering plane.

As can be seen from Table 2 our IHW post perihelion observations correspond to a phase when the sun-comet-earth angle increased to a maximum of  $66^{\circ}.1$  and remained there for next few days. In fact the phase angle on 17 Mar was  $65^{\circ}.9$  which is also very close to the maximum phase angle value.

The linear polarization measurements of this comet have been made by several other authors during the recent apparition (Bastien et al., 1986; Kikuchi et al., 1987; Le Borgne et al., 1987b; Dollfus et al., 1987 etc). We have plotted the linear polarization values as observed by them along with our observed polarization values at the three continuum filters centered at

0.365, 0.484 and 0.684  $\mu\text{m}$ , in Figures 3, 4 and 5 respectively. As a result we have observations from various sources covering a wide range of scattering angle almost from  $110^\circ$  to  $180^\circ$ . The features observed from Figures 3, 4 and 5 are: (1) except at low phase angle ( $180^\circ - \text{scattering angle}$ ) the polarization is always positive. The cross over from positive to negative polarization occurs at the scattering angle of  $160^\circ \pm 10^\circ$ . (2) the polarization seems to increase with wavelength when the phase angle is high.

### Section 6.3 Cometary grain properties

In the following we make an attempt to find the size distribution and complex values of refractive indices of the grains, which will fit to these observed values of polarization at different wavelengths. The dust mass detectors on board Vega and Giotto spacecrafts, have already found out the dust mass distribution functions (Mazets et al., 1987, McDonnell et al., 1986) of comet P/Halley. Assuming that the grains are spherical in size and the density of the grain particle  $\sim 1 \text{ gm/cc}$ , the following dust size distribution functions are those obtained by Mukai et al. (1987) from the in situ measurements (Mazets et al., 1987)

$$n(s) \sim s^{-2} \quad \text{where} \quad s < 0.62 \text{ } \mu\text{m}$$

$$n(s) \sim s^{-2.75} \quad \text{where} \quad 0.62 < s < 6.2 \text{ } \mu\text{m}$$

$$n(s) \sim s^{-3.4} \quad \text{where} \quad 6.2 < s \text{ } \mu\text{m}$$

where  $s$  is the radius of the grain in micron and  $n(s)$  is the number of grains having radius  $s$ . Krishna Swamy and Shah (1988) have discussed about the particle size limit for the reddening and

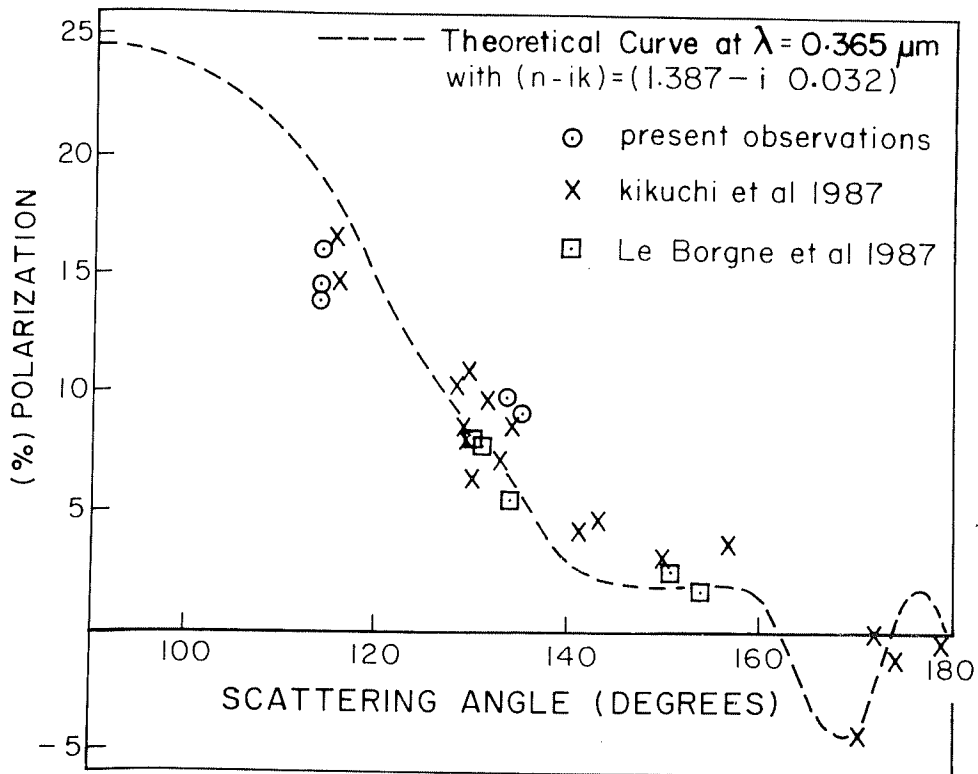


Figure3. Polarization values as observed at wavelength  $\lambda = 0.365 \mu\text{m}$  by different investigators are plotted along with the different scattering angles ( $= 180^\circ - \text{phase angle}$ ). The dashed curve has been fitted by the method of least square to the observed polarization data for complex value of refractive index  $(1.387 - i0.032)$ .

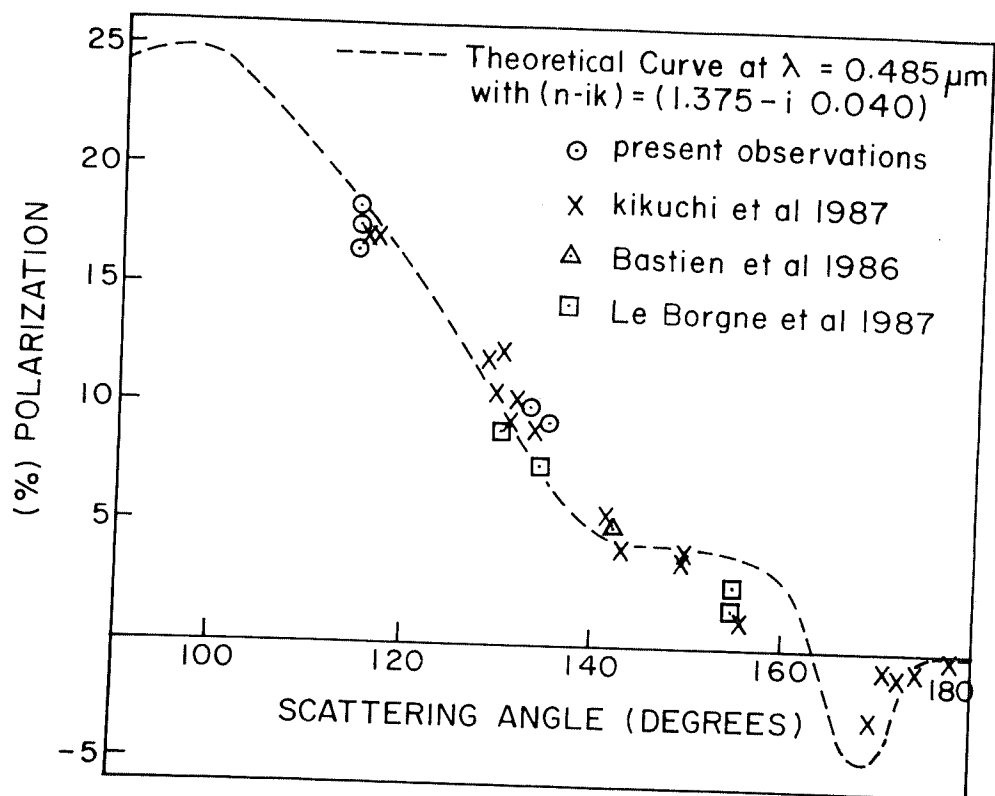


Figure 4. Polarization values as observed at wavelength  $\lambda = 0.484 \mu\text{m}$  by different investigators are plotted along with the different scattering angles ( $= 180^\circ - \text{phase angle}$ ). The dashed curve has been fitted by the method of least square to the observed polarization data for complex value of refractive index  $(1.375 - i0.040)$ .

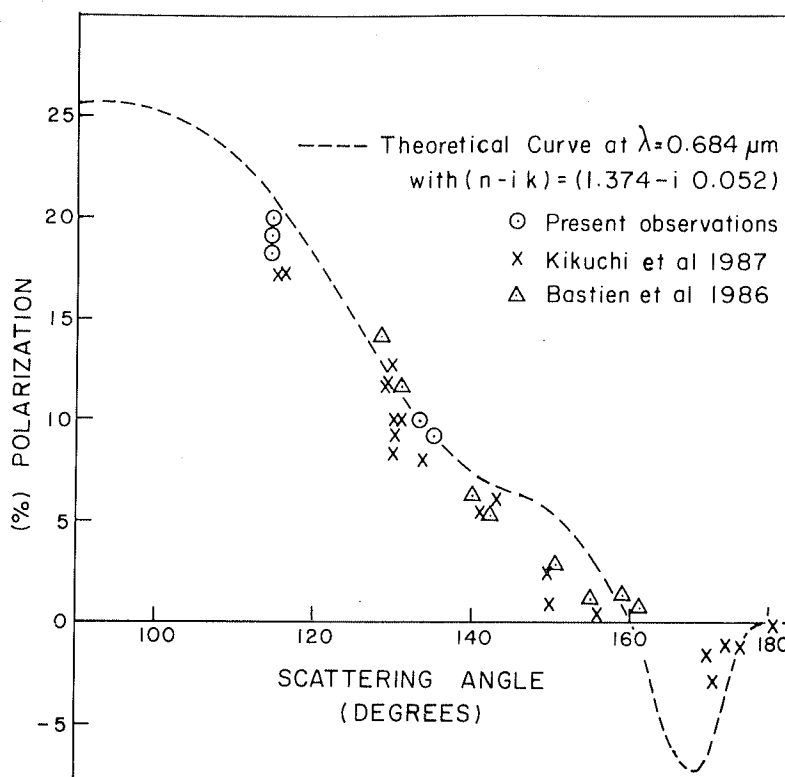


Figure 5. Polarization values as observed at wavelength  $\lambda = 0.684 \mu\text{m}$  by different investigators are plotted along with the different scattering angles ( $= 180^\circ - \text{phase angle}$ ). The dashed curve has been fitted by the method of least square to the observed polarization data for complex value of refractive index  $(1.374 - i0.052)$ . The observations taken by Kikuchi et. al. (1987) actually correspond to the wavelength value  $\lambda = 0.67 \mu\text{m}$  (Please see text).

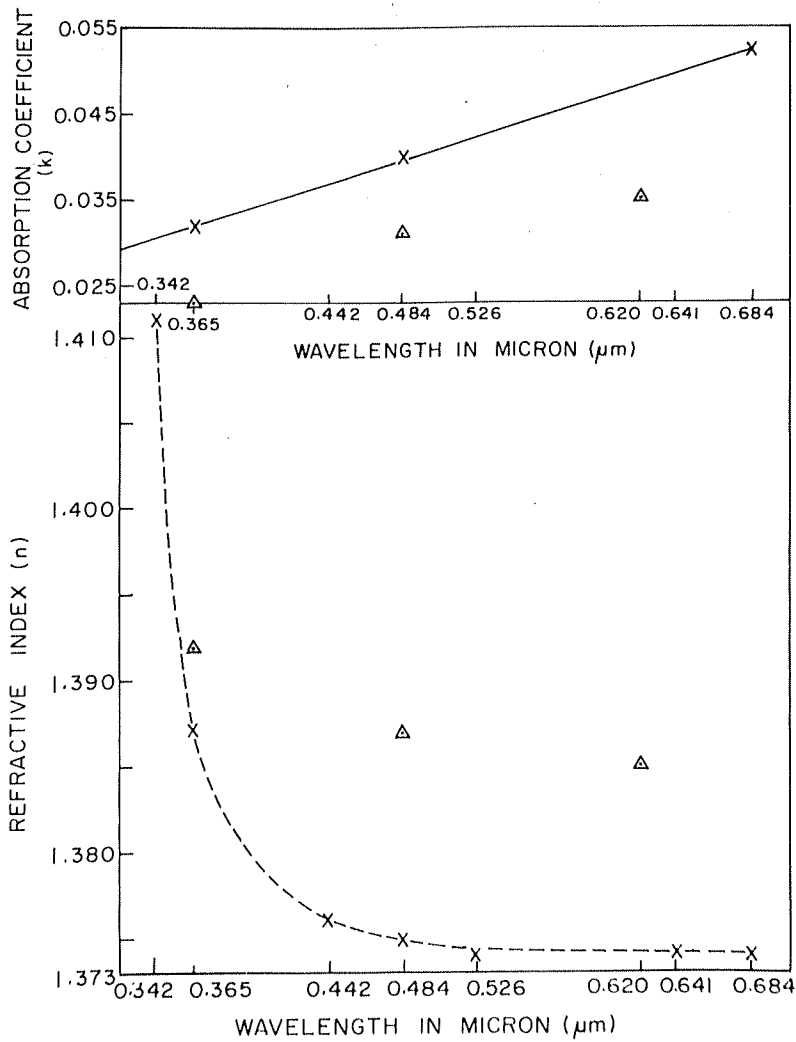


Figure 6. Different  $n$  and  $k$  values (marked by X) as obtained from the least square fit are plotted across different wavelengths. The  $k$  values have been joined by a solid line of best fit, where the  $n$  values have been joined by a dashed curve by free hand. The similar values obtained by Mukai et al.(1987) are shown along with (marked by  $\Delta$ ).



polarization calculations. From Krishna Swamy and Shah (1988) we have adopted the lower limit of particle size to be  $0.001 \mu\text{m}$ , for carrying out the Mie scattering calculations. Also from the same work, we have chosen the upper limit in the grain size to be  $20.0 \mu\text{m}$ , as grains bigger than this do not contribute effectively to the observed polarization. Having the grain size distribution fixed, we explored a wide range of  $(n-ik)$  values to calculate the expected values of polarization using Mie scattering formulations. For the phase angle values at which polarizations have been already observed, we have calculated the expected values of polarization and then calculated the sum of square of the difference between the observed and expected polarization values. Now by varying the values of  $(n-ik)$ , we found out the best fit value of  $(n-ik)$  for which the above sum becomes minimum. We introduce a quantity  $\sigma^2$  which is equal to the above sum divided by the number of data points. Thus at  $\sigma_{\min}$  we get the best fit value of  $(n,k)$ . The value of  $\sigma$  gives the confidence level on our best fit value of  $(n,k)$ . While doing these calculations we included the observed polarization values reported by several authors ( Bastien et al., 1986; Dollfus et al., 1987; Kikuchi et al., 1987; Le Borgne et al., 1987b) as can be seen from Figures 3, 4 and 5. These polarization values have been observed through different apertures and therefore a normalization of these values may be necessary. But as discussed earlier, since no definite trend of the aperture dependence of polarization has been established, we have not made any attempt to normalize these values. Another point to be noted here is that for  $\lambda=0.684 \mu\text{m}$  there are no polarization values available in the literature for this comet at a scattering

angle  $> 160^\circ$ . However, Kikuchi et al.(1987) have reported negative polarization measurements of this comet at  $\lambda=0.67 \mu\text{m}$  at phase angles  $> 160^\circ$ . Therefore while making the least square fit we have made use of the negative polarization values of the comet observed at  $\lambda=0.67\mu\text{m}$  reported by Kikuchi et al (1987). The positive polarization values observed by Kikuchi et al.(1987) at  $\lambda=0.67 \mu\text{m}$  are also plotted in Figure 5 along with all the other polarization values observed at  $0.684 \mu\text{m}$ , but have not been included in the calculation for  $(n-ik)$  at  $0.684 \mu\text{m}$ .

The important findings are the following set of complex values of refractive indices  $(n-ik)$  at the three discrete wavelengths which fit to the observed polarization data.

$(n-ik)$  is  $(1.387-i 0.032)$  at  $0.365 \mu\text{m}$  with  $\sigma = 2.9$   
 $(1.375-i 0.040)$  at  $0.484 \mu\text{m}$  with  $\sigma = 1.6$   
 $(1.374-i 0.052)$  at  $0.684 \mu\text{m}$  with  $\sigma = 2.4$ .

In Figure 6. we have plotted the above  $n$  and  $k$  values with the wavelength. All the  $k$  values can be fitted into a straight line ' $k = 0.062 \lambda + 0.009$ ' by the method of least square (vide Figure 6). The dependence of  $n$  on the wavelength seems to be nonlinear. Apart from the IHW filter polarimetry, we also have the polarimetric information on this comet at the continuum wavelength  $0.342$ ,  $0.442$ ,  $0.526$  and  $0.641 \mu\text{m}$  as listed in Table 1. Since these observations do not have good phase angle coverage, we do the following exercise to look into the nature of  $n-\lambda$  dependence more closely, which is otherwise not possible only from the three data points, defined by the IHW filters.

From the  $k$ - $\lambda$  straight line, we interpolate the  $k$  values at the wavelengths 0.342, 0.442, 0.526 and 0.641  $\mu\text{m}$  and list them in Table 3. Keeping these  $k$  values fixed, we try to find out the  $n$  values which can generate the polarization values as close as possible to the observed polarization values. These  $n$  values are also tabulated in Table 3. As a result we get more data points along the  $n$ - $\lambda$  curve, which now help us to see the  $n$ - $\lambda$  dependence in more detail. We have plotted the new set of  $n$  values in Figure 6 and the different points are joined by a dashed curve. Finally in Table 3 we put the actual observed polarization values, along with the polarization values calculated by using these set of  $(n-ik)$  values. The observed values of polarization seem to match very well with the theoretically calculated values for most of the cases as is clear from Table 3.

Mukai et al.(1987) have also found out the  $\lambda$ -dependence of the two parameters  $n$  and  $k$ . For a comparison we have also plotted their  $n$  and  $k$  values (marked by  $\Delta$ ) in Figure 6. At a particular wavelength their  $n$  value seems to be higher than our  $n$  value and  $k$  value seems to be lower than our  $k$  value. Apparently there seem to be no reasons for the difference between our set and their set of  $(n-ik)$  values. However, from the work by Mukai et al.(1987) it was not clear what were the upper and lower size limit of grain distributions they have used for the calculation of  $(n-ik)$ . If the size limits are different it may give rise to different  $(n-ik)$  values for the two cases. As an example in Table 4. we have compared the polarization values at different scattering angles, with two different particle size ranges 0.001-20.0 and 0.01-20.0  $\mu\text{m}$ . Moreover in order to fit the observed polarization data to the

Table 5. Percent polarization (P), error in percent polarization ( $\epsilon_p$ ), and position angle ( $\theta$ ) in degrees in the three continuum filters for coma and tail, as observed on 19 Mar.

		U	B	R
		0.365	0.484	0.684
COMA	P	13.89	16.67	18.24
	$\epsilon_p$	1.4	0.2	0.5
	$\theta$	165.1	166.2	165.0
TAIL	P	9.38	14.29	18.99
	$\epsilon_p$	1.5	0.6	1.0
	$\theta$	164.1	167.1	171.3

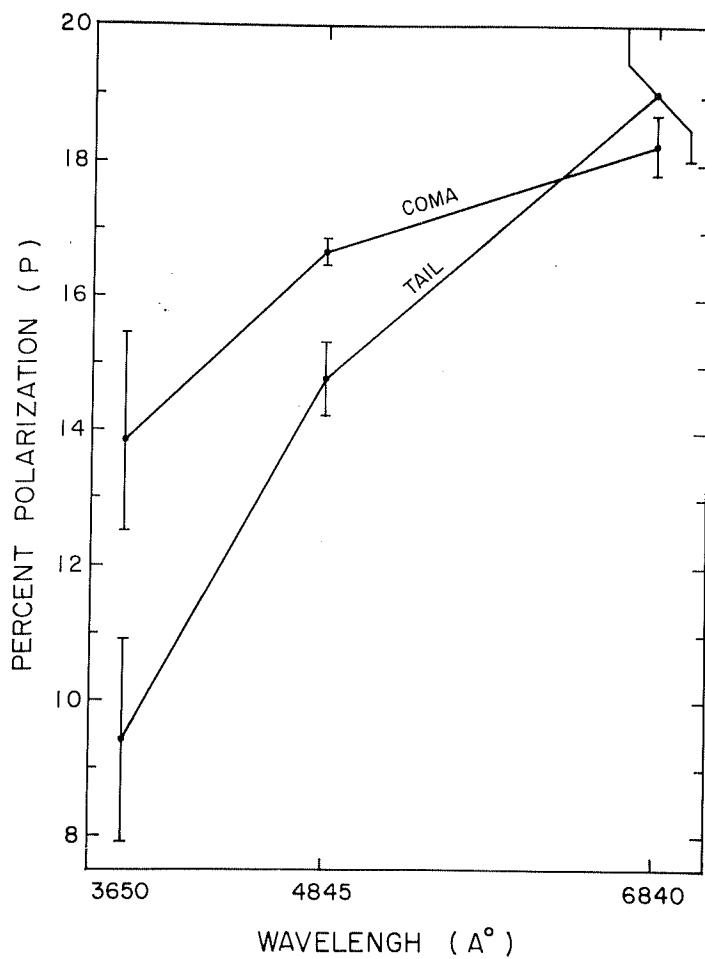


Figure 7. Wavelength dependence of linear polarization for coma and tail of comet P/Halley, as observed on 19 Mar 1986.

obtained by Mazets et al. (1987) explains the observed degree of polarization of comet P/Halley at different phase angles for particular kind of grains whose properties have been discussed above.

#### Section 6.4 Observation on 19 March

The observation on 19 March has a special significance, since it was taken for two regions in the comet. An entrance aperture of 24" diameter, corresponding to a linear size of about  $1.4 \cdot 10^4$  km on the comet, was used to observe (i) the central region of the coma (which has been already discussed) and (ii) another region across the dust tail, changing the RA and DEC each by  $-66''.6$  from the center of the coma. Henceforth, the second region will be referred as tail.

The degree of polarization ( $P$ ), error in polarization ( $\epsilon_p$ ), and position angle ( $\theta$ ) for coma and tail region are listed in Table 5. The degree of polarization increases with wavelength, both in coma and tail region (Figure 7). The coma is found to be more polarized than the tail at 0.365 and 0.484  $\mu\text{m}$ , whereas at 0.684  $\mu\text{m}$  the error bars overlap. Also it is noticed that the nature of wavelength dependence of polarization is different for coma and tail. This is probably due to the varying distribution of dust particles, the coarser ones being in the central regions of coma. Such segregation of grain sizes are possible, as has been discussed in chapter 5.

The position angle is found to be independent of wavelength and also perpendicular (within the errors) to the scattering plane.

## References

- Bastien, P., Menard, F., and Nadeau, R.: 1986, Monthly Notices Roy. Astron. Soc. 223, 827
- Brooke, T.Y., Knacke, R.F., and Joyce, R.R.: 1987, Astron. Astrophys. 187, 621
- Dollfus, A., Bastien P., Le Borgne, J.-F., Levasseur-Regourd, A.C., and Mukai, T.: 1988, Astron. Astrophys. 206, 348.
- Dollfus, A., and Suchail J.L.: 1987, Astron. Astrophys 187, 669
- Eaton, N., Scarrot, S.M., and Warren-Smith R.F.: 1988, Icarus 76, 270
- Kikuchi, S., Mikami, Y., Mukai, T., Mukai, S., and Hough, J.H.: 1987, Astron. Astrophys. 187, 689
- Krishna Swamy, K.S., and Shah, G.A.: 1988, Monthly. Notices. Roy. astron. Soc. 233, 573
- Lamy, P.L., Grun, E., and Perrin, J.M. : 1987, Astron. Astrophys. 187, 767
- Le Borgne, J.F., Leroy, J.L., and Arnaud, J.: 1987a, Astron. Astrophys. 173, 180
- Le Borgne, J.F., Leroy, J.L., and Arnaud, J. : 1987b, Astron. Astrophys. 187, 526
- Mazets, E.P., Sagdeev, R.Z., Aptekar, R.L., Golenetskii, S.V., Guryan, Yu.A., Dyachkov, A.V., Ilyinskii, V.N., Panov, V.N.,

Petrov, G.G., Savvin, A.V., Sokolov, I.A., Frederiks, D.D.,  
Khavenson, N.G., Shapiro, V.D., and Shevchenko, V.I. : 1987,  
Astron. Astrophys. 187, 699

McDonnell J.A.M., Alexander, W.M., Burton, W.M., Bussoletti, E.  
Clark, D.H., Grard, R.J.L., Grun, E., Hanner, M.S., Hughes., D.W.,  
Igenbergs, E., Kuczera, H., Lindblad, B.A., Mandeville, Minafra,  
A., Schwehm, G.H., Sekanina, Z., Wallis, M.K., Zarnecki, J.C.,  
Chakaveh, S.C., Evans, G.C., Firth, J.G., Littler, A.N., Massonne  
L., Olearczyk, R.E., Pankiewicz, G.S., Stevenson, T.J., and  
Turner, R.F.: 1986, Nature. 321, 338

Metz, K., and Haefner, R.: 1987, Astron. Astrophys. 187, 539

Mukai, T., Mukai, S., and Kikuchi, S.: 1987, Astron. Astrophys.  
187, 650

Sen, A.K., Joshi, U.C., Deshpande, M.R., Kulshretha, A.K., Babu,  
G.S.D., and Shylaja, B.S.: 1988, Astron. Astrophys. 204, 317

Sen, A.K., Joshi, U.C., and Deshpande, M.R. : 1989, Astron.  
Astrophys., 217, 307

Sen, A.K., Joshi, U.C., Deshpande, M.R., and Debi Prasad, C:  
1990, Icarus (in press).



## C H A P T E R 7

### Polarimetry of some interesting astronomical objects

#### Section 7.1 Variation of linear polarization in R Aquarii system

R Aquarii is a symbiotic system which embodies a number of characteristic properties that distinguish it from other peculiar stars. The visual spectrum indicates the presence of a cool Mira variable (period about 387 days) in close association with a hot unresolved ionizing source of radiation that appears to be responsible for the higher excitation nebular emission (Merrill 1950, Wallerstein and Greenstein 1980). Encircling this spatially unresolved ionized region is an extended ring-like nebula which extends to about 60" east and 75" west of the star, and this nebulosity moves outward (Hubble 1943; Baade 1944). Also there is a nebulosity much closer to the star, which to some extent is variable in brightness and structure; it tends to be extended north and south of the star at right angles to the outer arcs. R Aqr indicates the existence of a "jet-like" feature (hereafter referred to as a jet) of about 6" with a position angle of  $29^\circ$  from the central star (Sopka et al, 1982; Maun et al. 1985). Observations by Kafatos et al. (1983) reveal two discrete knots of emission—one at a distance of about 6" and the other at 2"-3" from the central object with P.A. of about  $29^\circ.3$  and  $45^\circ$ , respectively. IUE observations indicate that a hot ionizing source of radiation in the central object, probably a subdwarf, is responsible for the intense line and continuum radiation observed (Johnson 1982; Michalitsianos, Kafatos, and Hobbs 1980). Several models have

recently been advanced to explain the appearance of the emission features of R Aqr. Kafatos and Michalitsianos' (1983) model invokes supercritical mass exchange at periastron between the tenuous envelope of the Mira and a hot subdwarf moving in a highly eccentric ( $0.84 \leq e \leq 0.92$ ) orbit with a 44-year period. Spergel et al. (1983) have suggested a different model. According to their model, discrete clumps form in the neutral stellar winds of the Mira variable which are eventually illuminated and excited by the UV flux from the orbiting companion when these clumps enter the Strömgren volume.

Linear polarization measurements are important in understanding the peculiar geometry of the material surrounding the central object and the jet associated with the subdwarf. Wavelength and time dependence of polarization can be used to put constraints on the geometry of the object and to identify the mechanism(s) responsible for the polarization. In view of this, we have carried out linear polarization measurements of R Aqr in the UBVRI bands. Our observations give additional support for a binary model for the R Aqr system and suggest precision of the jet.

#### Section 7.1.1 Observations

Observations were made during November-December 1984 on the one meter telescope of the Indian Institute of Astrophysics, Kavalur with a two channel photopolarimeter discussed in chapter 2. The filter system is UBVRI. Measured values of percent polarization (P) and position angle ( $\theta$ ) at different phases, and earlier observations of Serkowski (1974) and Ladbeck (1985), are listed in Table 1.

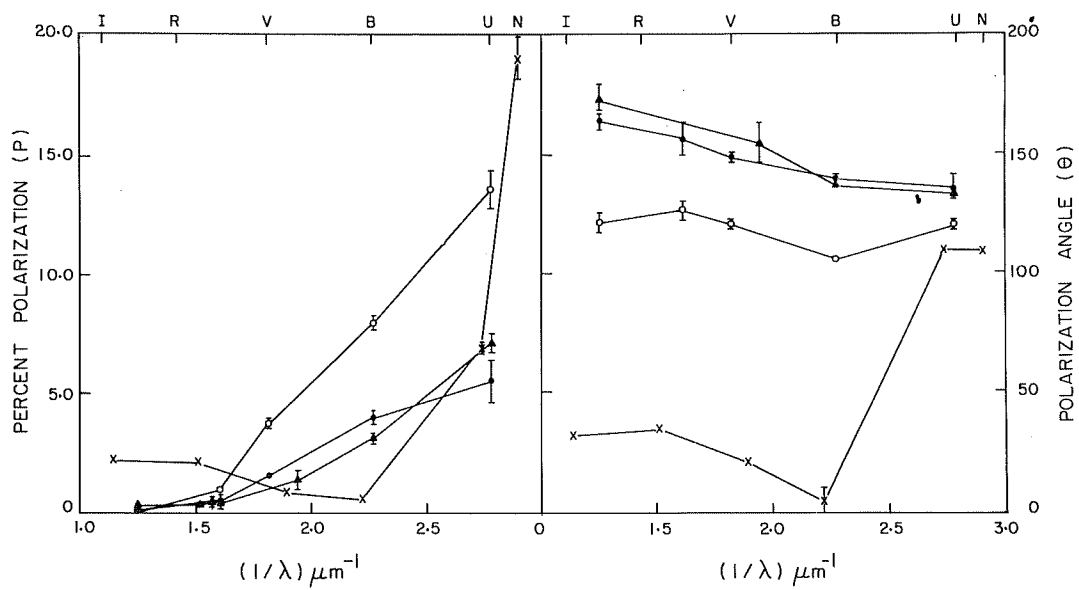


Figure 1. Polarization and position angle plots. Cross correspond to Serkowski(1974); filled triangle Ladbeck (1983); filled circle present data (Nov 1984); and open circle present data (Dec 1984).

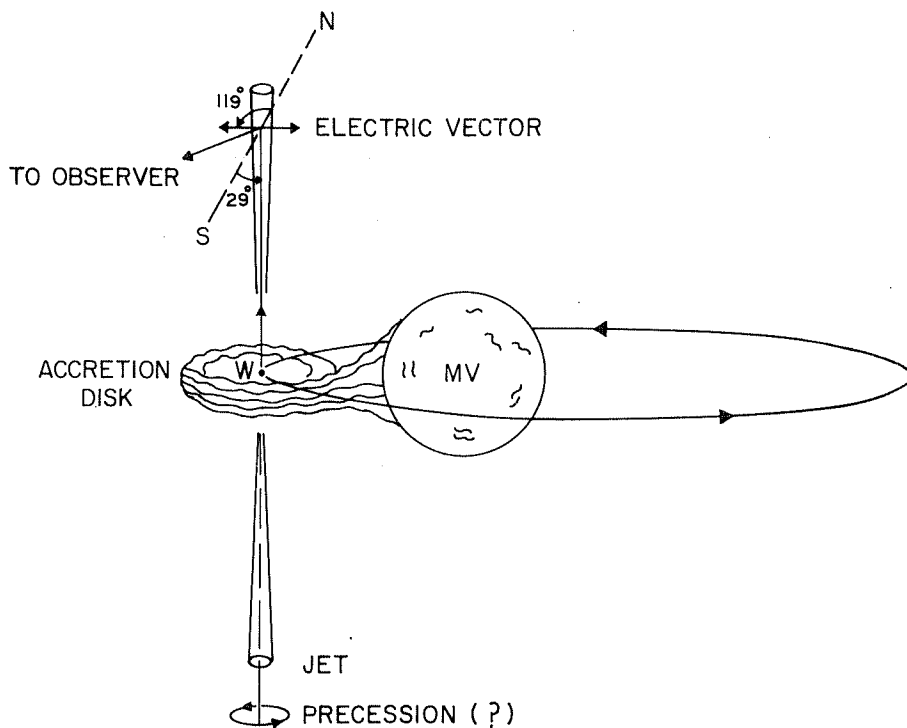


Figure 2. The binary model for the R Aqr system. MV is the mira variable, and W is the subdwarf. The high polarization in UV arises due to scattering of the light of the subdwarf from the material in the jets, whereas in the R and I bands the main contribution of the polarization comes from scattering in the circumstellar shell around the Mira variable..

### Section 7.1.2 Discussion of results

Figure 1 shows the observed wavelength dependence of linear polarization in the UBVRI bands at different phases. Observations of Serkowski (1974) and Ladbeck (1985) are also plotted for comparison. It is clear from the figure that the R Aqr shows strong wavelength and time dependence of polarization and position angle. As R Aqr is comparatively near to us (about 200 pc) and is located at high galactic latitudes ( $-70^\circ$ ), the interstellar polarization is expected to be negligible. Hence the observed large percent of polarization and its variation with time are intrinsic to R Aqr. In Figure 1 we see several interesting features in the percent polarization (P) as well as in the position angle ( $\theta$ ): (a) In the ultraviolet the polarization is large and varies between 5.37% to 19%. The data, as indicated in Table 1, were obtained between 1974 and 1984. These data show short term (one month) as well as long term (ten year) variations in P. (b) The position angle in the ultraviolet has remained unchanged at an angle of about  $120^\circ$ , though small variations with time are observed. (c) The polarization in the VRI bands is small (between about 0.5% to 7%). (e) The position angle in the VRI bands, unlike in the U band, show large changes ranging from  $20^\circ$  to  $170^\circ$ .

All of these observations support, and may be explained through, the binary model for the R Aqr system in which a hot subdwarf is orbiting around a Mira variable. When the white subdwarf is close to the periastron, mass transfer from the Mira variable takes place with the formation of a disk around the white subdwarf. When the mass accretion exceeds a critical limit, jet

Table 1. Polarimetric observations of R Aquarii

Date	Filter	$\lambda_{\text{eff}}$ ( $\mu\text{m}$ )	P (%)	$\epsilon_p$ (%)	$\theta$ ( $^\circ$ )	$\epsilon_\theta$ ( $^\circ$ )	References
14 Oct, 1974	N	0.345	19.00	0.9	108	1	Serkowski, 1974
	U	0.365	6.80	0.2	109	1	
	B	0.450	0.50	0.1	3	6	
	V	0.530	1.79	0.1	20	1	
	R	0.660	2.14	0.1	34	0.4	
	I	0.880	2.25	0.1	31	0.2	
Sep28-Oct17, 1983	U	0.360	7.00	0.5	133	2	Ladbeck, 1985
	B	0.440	4.02	0.2	137	1	
	OIII	0.514	1.34	0.4	154	8	
	Cont.						
	TiO	0.622	0.39	0.3			
	H $_{\alpha}$	0.636	0.43	0.2			
	Cont.						
	H $_{\alpha}$	0.657	0.28	0.1			
Nov2, 1984	RK	0.798	0.35	0.1			Present Obs.
	U	0.36	5.37	1.0	136	5	
	B	0.44	3.96	0.3	139	2	
	V	0.55	1.50	0.1	148	2	
	R	0.62	0.44	0.1	156	7	
	I	0.80	0.23	0.0	164	4	
Dec19, 1984	U	0.36	13.56	0.9	120	2	Present Obs.
	B	0.44	3.96	0.3	105	1	
	V	0.55	1.50	0.2	122	2	
	R	0.62	0.44	0.1	126	4	
	I	0.80	0.23	0.0	121	4	

structures are formed (Kafatos and Michalitsianos 1982). The optical and radio observations (Sopke et al. 1982; Hollis et al. 1985) of R Aqr indicates the existence of a jet. When the gas in the jet is heated by intense UV radiation from the white subdwarf, a high degree of polarization arises due to Thompson scattering. This explains the observed feature (a) above. The observed jet has a position angle  $29^\circ$  (Sopka et al. 1982). If the polarization in the U band arises from the jet one would get a value of  $119^\circ$  as given in Table 1. This explains the observed feature (b) above. The small variation in position angle in the U band around the expected value of  $119^\circ$  may be due to precision of the jet around an axis; however more data are required to confirm this. The above findings indicate that the effects observed in the ultraviolet are mainly due to the white subdwarf. As we come to the longer wavelengths, especially in the R and I bands, it appears that the main contribution comes from the mira variable. The polarization in these bands may be due to the dust shell around the R Aqr system (as observed in (c) above). The large changes in position angle at the V, R, and I bands may be due to changes in the nebulosity around the R Aqr system.

The above findings strongly suggest that R Aqr has a Mira variable around which a white subdwarf is moving in an elliptical orbit. Close to periastron, the white dwarf accretes material from the Mira variable. A jet-like structure is formed when the accretion exceeds a critical value. It is likely that the jet may be precesing (Figure 2). Though the model proposed by Spergel Et al. (1983) explains most of the features we have observed (a, c, d, and e), it fails to explain feature (b) -- ie, the position

angle in UV remains almost unchanged. Further observations are needed to explore (a) whether polarization and the orbital period of the white subdwarf have any correlation, (b) whether the jet weakens at apastron, (c) whether the jet precesses, and (d) whether a 387 day periodicity in the Mira variable has any correlation with the I band polarization.

## Section 7.2 Polarimetric investigations of some peculiar supergiants.

Stars HD161796(F3Ib), HD101584(FOIape) and HD163506/89 Her(F2Ipe) are F-supergiants and HD89353/HR4049(B9.5) is a hypergiant. All these stars are at high galactic latitude and their evolutionary stages are not clear. IRAS measurements show large IR excess in these stars (Parthasarathy and Pottasch, 1986; Lamers et al. 1986). Parthasarathy and Pottasch(1986) have attributed large IR excess in HD161796 and HD101584 due to substantial dust mass around them. Stars HD161796 and HD101584 emit almost as much energy in the far infrared as in the visible region of the spectrum (Parthasarathy and Pottasch, 1986). Star HR4049 besides large IR excess, shows severe UV deficiency (Humphrey and Ney, 1974a and b). Stars HD101584 and 89 Her have many similarities and both show 10  $\mu\text{m}$  silicate emission features (Humphrey and Ney, 1974a and b; Gillet et al. 1970). It is quite remarkable that there is no noticeable reddening for either HD161796 or HD101584. Humphrey and Ney (1974a and b) based on IR photometry have suggested that HD101584 and 89 Her are binary stars with cool companions. However, based on the study of velocity variations Burki et al. (1980) found no evidence of



binary nature of HD161796 and 89 Her. Star HR4049 shows about 0.4 mag variations in brightness in a time scale of 140 days (WaelkYo and Rufener, 1983). Other stars also show small amplitude light and radial velocity variations similar to long period cepheids (Ferne, 1981;1983).

To understand further, the peculiar behavior of these stars, polarimetric observations were undertaken and investigations are reported here.

#### Section 7.2.1.Observations and analysis

Observations were taken on one meter telescope of Indian Institute of Astrophysics, Kavalur, using our polarimeter which has been described in chapter 2. Filter system used was UBVR. Polarization measurements were made during the dark phase of moon and the difference between (sky + star) data and sky data is typically ~ 7 to 8 mag and sky polarization is ~ 6 to 7% in visual band. Therefore the polarization values are meaningful

The results of the observations for all stars observed for the present program are listed in Table 2, which contains the star name, JD of observation,  $P$ ,  $E_p$ ,  $\theta$  and  $E_\theta$ .

#### Section 7.2.2 Discussion of results

Figure 2 shows the wavelength dependence of  $P$  and  $\theta$ . From the figure it appears that  $P$  and  $\theta$  are almost independent of wavelength in the visual region of the spectrum except for HR4049(HD89353) and HD101584 for which the position angles show a change of  $67^\circ$  and  $20^\circ$  respectively from red to blue region. Polarization values for the program stars are less than 1% except

Table 2 Polarimetric observation of some peculiar supergiants. The numbers in brackets are error values.

star	Julian Date	$P_U$ 244650, %	$\theta_U$ ( $^\circ$ )	$P_B$ %	$\theta_B$ ( $^\circ$ )	$P_V$ %	$\theta_V$ ( $^\circ$ )	$P_R$ %	$\theta_R$ ( $^\circ$ )
HD89353 (HR4049)	5.24	0.39 (0.11)	179 (8)	0.30 (0.04)	34 (4)	0.33 (0.03)	66 (2.5)	0.45 (0.10)	59 (6)
HD101584	5.22	0.94 (0.10)	132 (3)	1.12 (0.04)	119 (1)	1.29 (0.03)	116 (1)	1.29 (0.01)	113 (1)
HD161796	4.34	0.60 (0.10)	117 (5)	0.57 (0.04)	117 (2)	0.60 (0.03)	110 (1.5)	0.50 (0.06)	107 (3.5)
HD163506 (89Her)	5.44			0.64 (0.04)	66 (2)	0.60 (0.05)	60 (3)	0.83 (0.07)	61 (2.7)

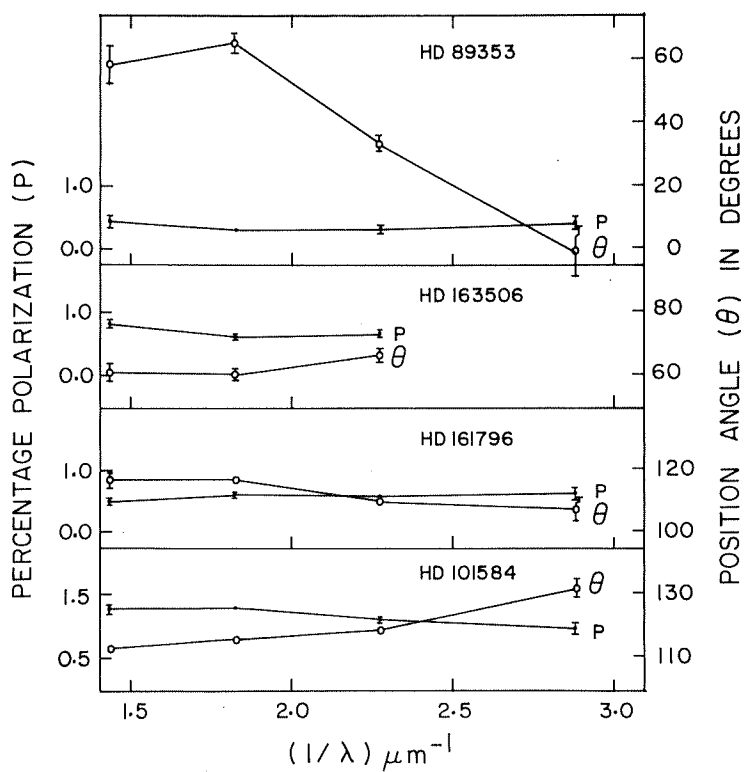


Figure 3. Wavelength dependence of percent polarization and position angle. Error bars are marked.

for HD101584 for which it is higher than 1%. Since all these stars are at high galactic latitude, the expected interstellar polarization is much less ( $< 0.2\%$ ) than the observed values. In addition the wavelength dependence of  $P$ , for all stars, is quite different compared to the interstellar polarization. Also the position angle for interstellar polarization is independent of wavelength, whereas in present case at least two stars show significant changes in  $\theta$ . Hence the observed polarizations are intrinsic to the stars. These observations along with large IR excess, but with almost negligible reddening (Parthasarathy and Pottasch, 1986; Lamers et al. 1986; Humphrey and Ney, 1974a and b) are discussed in the following:

The large infrared fluxes from these objects have been attributed to the massive dust shell around these stars (Parthasarathy and Pottasch 1968; Lamers et al. 1986). The degree of polarization in optical region is rather low which perhaps indicates almost spherically symmetric distribution of the dust around the stars. Since there are no observational evidence of polarization in F supergiants, we assume that the intrinsic radiation from the star to be unpolarized and the polarization is introduced by the scattering of light due to the circumstellar matter. All stars show weak wavelength dependence of polarization which is indicative of large dust particles ( $> 0.3 \mu\text{m}$  for silicate grains) in the circumstellar shell. The presence of large grains also explains the zero reddening (Drain and Lee, 1984) observed in the optical region for these stars (Humphreys and Ney, 1974a and b). Stars HD101584 and HR4049 show some additional features in their polarization curve (Figure 3) which can be

attributed to other characteristics associated with the dust shell. These two stars are discussed here in detail.

HD101584: This star shows a slow increase of polarization towards the red wavelength and also shows (Figure 3) wavelength dependence of polarization angle, namely  $\theta$  decreases by  $\sim 20^\circ$  from U band to R band. The error in position angle in U band is  $\sim 3^\circ$ . In other bands the error is much smaller than in U band (Table 2). Therefore, the change of  $20^\circ$  in position angle is quite significant. This is indicative of multilayer dust shell having grains of different sizes or there is a radial gradient in grain size. The IR spectrum shows that the infrared flux continuously increases with increasing wavelength up to  $100\ \mu\text{m}$  (Parthasarathy and Pottasch, 1986), which could be due to temperature gradient in the dust shell. This supports the view that the grain size changes radially. The degree of polarization shows a very slow increase towards the R band and attains a maximum value at R band or beyond this wavelength. Therefore the most typical grain size is expected to be about  $0.3\ \mu\text{m}$  (assuming silicate grains).

HD89353(HR4049): This star presents very interesting case. Earlier Mathewson and Ford (1970) have reported the polarization value of this star through B-filter. The present measurements show that the degree of polarization has weak wavelength dependence whereas the position angle shows strong wavelength dependence;  $\theta$  changes by  $\sim 67^\circ$  from U band to R band (Figure 3). The change in  $\theta$  is much larger than the error in observation (Table 2). The observed degree of polarization has a minimum in the B band and

increases slowly towards shorter and longer wavelength. The nature of the observed wavelength dependence of polarization and position angle is quite different than the usual interstellar polarization. Therefore the radiation from the star is intrinsically polarized, though the observed polarization contains a mixture of interstellar polarization. However, the contribution of interstellar polarization is expected to be much less than the observed polarization as the star is located at high galactic latitude ( $b=22^{\circ}.5$ ). The interstellar polarization for this star has been estimated as follows. Interstellar extinction for this star is small (Mathewson and Ford, 1968). We have adopted extinction  $\sim 0.2$  mag., which corresponds to a polarization value  $\sim 0.2\%$  (assuming  $P/A_V = 0.025$  (Greenberg, 1978)). Therefore, we adopt  $P_{\text{max}}(\text{interstellar}) \sim 0.2\%$  and  $\theta(\text{interstellar}) = 75^{\circ}$  (Mathewson and Ford, 1970) for the direction of this star. Further we have adopted the interstellar polarization law;  $P/P_{\text{max}} = \exp(-K \ln^2(\lambda_{\text{max}}/\lambda))$  (Serkowski, 1975) with  $\lambda_{\text{max}} = 0.55 \mu\text{m}$ . The corrected values of the observed polarization have been obtained by subtracting vectorially the interstellar polarization values from the observed values. The polarization values in UBV bands thus obtained are respectively 0.45, 0.31, 0.14 and 0.27 percent and the respective position angles are  $99^{\circ}$ ,  $162^{\circ}$ ,  $26^{\circ}$  and  $24^{\circ}$ . This again shows that the position angle flips near B band. Also the degree of polarization increases on both the sides of BV bands.

One possible explanation for this kind of wavelength dependence could be based on two shell model - one shell containing small particles and the other containing large dust particles. The net polarization is the result of the superposition of polarization

produced by two shells. Assuming silicate grains of refractive index  $m=1.66$  and the extinction efficiencies given by Greenberg (1978), we infer that the smaller particles are of the size  $0.05\ \mu\text{m}$  and bigger particles being  $0.8\ \mu\text{m}$ . The symmetry axis of two shells should be different to produce the flip in the position angle. Based on the energy distribution from  $0.155\ \mu\text{m}$  to  $100\ \mu\text{m}$  Lamers et al. (1984) have also concluded to the presence of two kinds of particles - small size particles being  $0.05\ \mu\text{m}$  and larger particles being  $1\ \mu\text{m}$ . Our finding also gives the similar results. Lamers et al. (1984) have also suggested the possibility of spherically asymmetric shell around the star. However, the polarization observations cannot be explained only on the basis of spherically asymmetric shell. The comparison of the present polarization measurements with the values reported earlier by Mathewson and Ford (1970) in B filter does not show variation. This perhaps reinforces the possibility of single star surrounded by two dust shells.

## References

- Baade, W.A.: 1944, Ann. Rep. Dir. Mount Wilson Obs. 1943-44, 12.
- Burki, G., Mayor, M., and Rufener, F.: 1980, Astron. Astrophys. Suppl. 42, 383.
- Draine, B.T., and Lee, H.M.: 1984, Astrophys. J. 285, 89.
- Fernie, J.D.: 1981, Astrophys. J. 243, 576.
- Fernie, J.D.: 1983, Astrophys. J. 265, 999.
- Fitzgerald, M.P.: 1968, Astron. J. 73, 988.
- Gillett, F.C., Hyland, A.R., and Stein, W.A.: 1970, Astrophys. J. Letters 162, L21.
- Greenberg, J.M. :1978, in Cosmic Dust, J.A.M. McDonnell, Ed. Wiley, p.187
- Hall, J.S., and Serkowski, K.: 1963, Basic Astronomical Data, K. Strand, Ed. (Chicago, Univ. of Chicago Press), Ch.16
- Herbig, G.H.: 1972, Astrophys. J. 172, 375
- Hollis, J.M., Kafatos, M., Michalitsianos, A.G., and McAlister, H.A.: 1985, Astrophys. J. 289, 765.



Hubble, E.P.: 1943, Ann. Rep. Dir. Mount Wilson Obs. 1942-43, 17.

Humphreys, R.M., and Ney, E.P.: 1974a, Astrophys. J. Letters 187, L75

Humphreys, R.M., and Ney, E.P.: 1974b, Astrophys. J. 190, 339

Johnson, H.M.: 1982, Astrophys. J. 253, 224.

Kafatos, M., and Michalitsianos, A.G.: 1982, Nature 298, 540.

Kafatos, M., Hollis, J.M., and Michalitsianos, A.G.: 1983, Astrophys. J. Letters 267, L103.

Ladbeck, R.S.: 1985, Astron. Astrophys. 142, 333.

Lamers, H.J.G.L.M., Waters, L.B.F.M., Garmany, C.D., Perez, M.R., and Waelkens, C.: 1986, Astron. Astrophys. 154, L20.

Mathewson, D.S., and Ford, V.L.: 1970, Mem. Roy. Astron. Soc. 74, 139.

Mauron, N., Nieto, J.L., Picat, J.P., Lelievre, G., and Sol, H.: 1985, Astron. Astrophys., 142, L13.

Merril, P.W. :1950, Astrophys. J. 112, 524.

Michalitsianos, A.G., Kafatos, M., and Hobbs, R.W.: 1980,

Astrophys. J. 237, 506.

Parthasarathy, M., and Pottasch, S.R.: 1986, Astron. Astrophys. 154, L16.

Serkowski, K.: 1974, IAU Circular, No 2712.

Serkowski, K., Mathewson, D.S., and Ford, V.L.: 1975, Astrophys. J. 196, 261.

Sopkaq, R.J., Herbig, G., Kafatos, M., and Michalitsianos, A.G.: 1982, Astrophys. J. Letters 258, L35.

Spiegel, D.N., Giuliani, J.L., Jr., and Knapp, G.R.: 1983, Astrophys. J. 275, 330.

Waelkens, C., and Rufener, F.: 1983, Hvar Obs. Bull. 7, No.1, 29

Wallesterstein, G., and Greenstein, J.L.: 1980, Pub. Astro. Soc. Pac. 92, 275.